Hydrodynamic modes as singular eigenstates of the Liouvillian dynamics: Deterministic diffusion

Pierre Gaspard
Centre for Nonlinear Phenomena and Complex Systems, Université Libre de Bruxelles, Campus Plaine, Code Postal 231, B-1050 Brussels, Belgium
(Received 2 August 1995)

Hydrodynamic modes of diffusion and the corresponding nonequilibrium steady states are studied as an eigenvalue problem for the Liouvillian dynamics of spatially extended suspension flows which are special continuous-time dynamical systems including billiards defined on the basis of a mapping. The infinite spatial extension is taken into account by spatial Fourier transforms which decompose the observables and probability densities into sectors corresponding to the different values of the wave number. The Frobenius-Perron operator ruling the time evolution in each wave number sector is reduced to a Frobenius-Perron operator associated with the mapping of the suspension flow. In this theory, the dispersion relation of diffusion is given as a Pollicott-Ruelle resonance of the Frobenius-Perron operator and the corresponding eigenstates are studied. Formulas are derived for the diffusion and the Burnett coefficients in terms of the mapping of the suspension flow. Nonequilibrium steady states are constructed on the basis of the eigenstates and are given by mathematical distributions without density functions, also referred to as singular measures. The nonequilibrium steady states are shown to obey Fick's law and to be related to Zubarev's local integrals of motion. The theory is applied to the regular Lorentz gas with a finite horizon. Generalizations to the nonequilibrium steady states associated with the other transport processes are also obtained.

PACS number(s): 05.40.+j, 05.20.Dd, 05.45+b

I. INTRODUCTION

Hydrodynamic modes have always played a central role in nonequilibrium statistical mechanics and in the description of irreversible processes [1–4]. The concept of the hydrodynamic mode establishes the interface between the description in terms of kinetic equations such as the Boltzmann equation and the macroscopic description in terms of the phenomenological equations such as the diffusion equation

$$\partial_t n = D\nabla^2 n, \tag{1}$$

where n is the fluid density (or concentration) and D is the diffusion coefficient. The importance of hydrodynamic modes holds in their property of being eigensolutions of the phenomenological equation. In the case of the diffusion equation, these modes are given by

$$n_{\mathbf{k}}(\mathbf{r},t) = \exp(s_{\mathbf{k}}t)\exp(i\mathbf{k}\cdot\mathbf{r}), \tag{2}$$

which describe periodic profiles of concentration characterized by the wave number $\mathbf{k}$. The hydrodynamic modes decay exponentially in time because the corresponding eigenvalues are real and negative,

$$s_{\mathbf{k}} = -Dk^2. \tag{3}$$

Accordingly, the concentration becomes spatially uniform and approaches the thermodynamic equilibrium in the long time limit ($t\to+\infty$).

This exponential decay to the thermodynamic equilibrium seems apparently incompatible with the microscopic Hamiltonian dynamics which is time reversible and which, moreover, preserves phase-space volumes. As a consequence, hydrodynamic modes have long been considered at the intermediate level of the approximate kinetic equations but not at the fundamental level of the exact Liouvillian equation describing the time evolution of probability densities ρ_t in phase space,

$$\rho_t(X) = \hat{P}^t\rho_0(X) \equiv \rho_0(\Phi^{-t}X), \tag{4}$$

where Φ^t represents the flow induced by the Hamiltonian H on the energy shell $H=E$ and $\hat{P}^t$ is the Frobenius-Perron operator.

The purpose of the present paper is to describe a theory in which this major difficulty is resolved. The theory is based on the concept of Pollicott-Ruelle resonances of the Frobenius-Perron operator ruling the time evolution of probability densities in phase space [5–8]. We extend the spectral theory of the Frobenius-Perron operator to diffusion in continuous-time dynamical systems which are spatially extended. The theory is developed by considering the continuous-time dynamical system as a so-called *suspension flow*, in which the flow is defined on the basis of a mapping and of a return time function. The mapping may be induced by the intersections of the trajectories with a Poincaré hypersurface of section. Billiards are particular examples of suspension flows because the trajectories are governed by the so-called Birkhoff mapping, which uniquely determines the successive elastic collisions. When the billiards are formed by a lattice of obstacles the point particle may undergo a process of deterministic diffusion, as is the case in the regular Lorentz gas with a finite horizon [9–12]. However, we emphasize that the present theory applies to a large class of spatially extended systems we define in the following, which includes not only billiards but also Hamiltonian systems. The following work has been motivated by recent results obtained by the author on the hydrodynamic modes of diffusion in the area-preserving multibaker map [13–16] (see also

[17], which describes a systematic application of these results to several other simple maps).

In the case of spatially extended systems which form a periodic lattice, spatial Fourier transforms are needed in order to reduce the dynamics to an elementary cell of the lattice, also called a Wigner-Seitz cell in solid-state theory [18]. In this reduction, a wave number $\mathbf{k}$ is introduced which characterizes the spatial periodicity of the observables and of the probability densities. Each Fourier component of the probability density evolves differently in time, which requires introduction of a new Frobenius-Perron operator depending explicitly on the wave number $\mathbf{k}$. Accordingly, the Pollicott-Ruelle resonances and the associated eigenstates also depend on the wave number $\mathbf{k}$, as expected for hydrodynamics modes like (2).

However, an essential difference appears between the case of the phenomenological equation (1) and the case of the Frobenius-Perron equation. This fundamental difference holds in the fact that the eigenstates corresponding to the Pollicott-Ruelle resonances are mathematical distributions or singular measures as shown by Ruelle [8]. The impossibility of constructing eigenstates in terms of functions has its origin in the pointlike character of the deterministic dynamics and in the property of dynamical instability. This aspect is closely related to the *Stosszahlansatz* of Boltzmann according to which the deterministic Liouville equation is approximated by a kinetic equation of stochastic character obeying an H theorem. The stochastic assumption introduces a global smoothing of the dynamics so that the eigenstates can be constructed in terms of functions, as is the case with the Fokker-Planck equation, for instance. However, in the absence of global stochastic smoothing, the eigenstates must in general be considered as distributions or singular measures, in which case their construction becomes possible at the level of the deterministic Liouvillian dynamics if the underlying system is hyperbolic, as carried out here below.

Therefore the introduction of singular measures in the statistical description of the dynamics allows the Frobenius-Perron operator to admit eigenstates corresponding to the hydrodynamic modes of relaxation toward equilibrium. The compatibility with time reversibility is established as follows. Hyperbolic systems have local stable and unstable manifolds which are the directions under which the exponential separation occurs under forward or backward time evolutions, respectively. Therefore an eigenstate $\mu^{(+)}$ which corresponds to the relaxation toward equilibrium for $t\rightarrow+\infty$ turns out to be smooth in the unstable direction but singular in the stable direction. Since the stable and unstable manifolds exchange their role under time reversal, the situation is reversed for the eigenstate $\mu^{(-)}$ which relaxes to equilibrium for $t\rightarrow-\infty$: this measure is smooth in the stable direction but singular in the unstable direction. The smoothness in the unstable direction is reminiscent of the property of the Sinai-Ruelle-Bowen measures to be absolutely continuous with respect to the Lebesgue measure in the unstable direction [19]. These results hold not only for billiards but also for general suspension flows and, as another possible example, for the Hamiltonian flow of a particle in a lattice of Yukawa potentials [20].

Here a word is in order about the comparison with other recent approaches involving singular measures. Singular measures may also arise when the support of the invariant or conditionally invariant measures are fractals of zero Lebesgue measure. This is the case in the chaotic-scattering approach where phase-space volumes are preserved but a fractal repeller is formed because the phase space is noncompact and sustains an escape process as recently described in detail by Gaspard and co-workers and Chernov and Markarian [21–26]. In the thermostatted-system approach, singular measures are generated because the dynamics does not preserve the volumes [27]. Here, we would like to emphasize that the measures we consider are singular although the dynamics preserves the volumes and the support is the plain phase space of positive Lebesgue measure. This particularity has its origin in the property of the Frobenius-Perron operator of spatially extended systems to depend on a wave number $\mathbf{k}$. Therefore the corresponding eigenstates $\mu^{(\pm)}$ also depend on the wave number and their singular character comes from the Bloch-type quasiperiodic boundary conditions [18]. The eigenstates become smooth in both the stable and the unstable directions only for the microcanonical measure which is obtained at vanishing wave number $\mathbf{k}=\mathbf{0}$.

The present work is the continuation of a previous work by Cvitanović, Eckmann, and Gaspard, who developed a periodic-orbit theory of diffusion [28]. In this context, the diffusion coefficient has been obtained in terms of the unstable periodic orbits of the dynamics in an elementary cell of the lattice. The formula was derived from the leading Pollicott-Ruelle resonance given by a zero of the ζ function of an appropriate Frobenius-Perron operator. We shall here consider a similar Frobenius-Perron operator, but one which is written explicitly for the corresponding suspension flow, which allows us not only to recover the results of periodic-orbit theory but also to obtain explicitly the associated eigenstates.

Moreover, we construct the nonequilibrium steady state corresponding to a gradient of concentration across the system. In the case of the phenomenological equation (1), such nonequilibrium steady states are given by

$$n_{\mathbf{g}}(\mathbf{r})=-i\mathbf{g}\cdot\frac{\partial}{\partial\mathbf{k}}n_{\mathbf{k}}(\mathbf{r},t)\big|_{\mathbf{k}=0}=\mathbf{g}\cdot\mathbf{r}, \tag{5}$$

which describes a linear profile of concentration across the system in the direction of the gradient $\mathbf{g}$. At the level of kinetic theory, the connection between the hydrodynamic modes and the nonequilibrium steady states has been the object of systematic studies, in particular, by Kirkpatrick, Cohen, and Dorfman [29]. For the model of the multibaker, such nonequilibrium steady states have recently been constructed at the level of the Liouvillian dynamics by Tasaki and Gaspard [30,31]. In this construction, a new term appears with respect to the phenomenological steady state (5) which has its origin in the fluctuations around the average linear profile. We show below that this result also holds in general spatially extended suspension flows and, in particular, in the regular Lorentz gas. In this regard, we notice that the Lorentz gas is not an Axiom-A system [9–11]. The induced mapping has lines of discontinuities so that the fields of stable and unstable directions are not continuous, which has for consequence that most of the global stable and unstable sets are not manifolds but only segments of manifolds.

This constitutes an important difference with respect to the multibaker map, which nevertheless does not prevent the construction of the nonequilibrium states on the basis of the same principles we used in previous works. Therefore the present generalization of our previous results shows that the singular character of the Liouvillian hydrodynamic modes is a general property of dynamically unstable systems.

The paper is organized as follows. Section II describes what we mean by suspension flows. In Sec. III a preliminary Frobenius-Perron operator is derived for the flow by using Fourier transforms to reduce the dynamics from the lattice to one of its elementary cells. The Frobenius-Perron operator of the mapping of the suspension flow is studied in Sec. IV together with the corresponding eigenvalue problem. The nonequilibrium steady states are obtained in Sec. V. The higher-order diffusion coefficients are studied in Sec. VI. The theory is applied to the Lorentz gas in Sec. VII where the eigenvalues, the eigenstates, and the nonequilibrium steady states are explicitly constructed. The results are summarized and conclusions are drawn in Sec. VIII.

II. STATISTICAL MECHANICS OF SUSPENSION FLOWS

A. Suspension flows of infinite spatial extension

We consider a dynamical system of infinite spatial extension in a phase space defined by the coordinates $X=(\mathbf{r},\mathbf{s}) \in \mathbb{R}^D$, where $\mathbf{r}\in\mathbb{R}^L$ are the position coordinates in which the system forms a Bravais lattice $\mathscr{L}$. The coordinates $\mathbf{s} \in \mathbb{R}^{D-L}$ are supplementary coordinates which are necessary to uniquely specify the initial condition of the trajectories. A lattice vector $\mathbf{l_m}$ is centered in each cell of the Bravais lattice, with $\mathbf{m}=(m_1,\ldots,m_L)\in\mathbb{Z}^L$. The lattice vectors are given as linear combinations of the basic vectors of the lattice

$$\mathbf{l_m}=m_1\mathbf{l}_{100\ldots00}+m_2\mathbf{l}_{010\ldots00}+\cdots+m_L\mathbf{l}_{000\ldots01}\in\mathscr{L}. \tag{6}$$

By using the invariance of the lattice dynamics under spatial translations, the flow Φ^t over the whole lattice can be reduced to a flow ϕ^t in one and the same elementary cell of the lattice. The flow ϕ^t may be further reduced to a mapping if a Poincaré hypersurface of section $\mathscr{P}$ is considered in the elementary cell

$$\xi_{j+1}=\varphi(\xi_j) \quad \text{with} \quad \xi_j\in\mathscr{P}, \tag{7}$$

and $\dim\mathscr{P}=D-1$.

We notice that the mapping alone does not provide a complete description of the flow because the coordinate along the direction of the flow has been eliminated by introducing the Poincaré hypersurface of section. To restore this information, the current phase-space position along the trajectory can be determined by the interval of time τ elapsed since the last passage in the hypersurface of section. This time τ takes its values in the range $0\leqslant\tau<T(\xi)$, where we have introduced the time of first return $T(\xi)$ in the hypersurface of section, which is the time between the intersections ξ and $\varphi(\xi)$ with $\mathscr{P}$. Under these assumptions, the complete phase space can be represented in the new coordinates

$$X=(\xi,\tau,\mathbf{l})\in\mathscr{P}\otimes[0,T(\xi)[\otimes\mathscr{L}. \tag{8}$$

In this phase space, the dynamics on the lattice is described by the following suspension flow Φ^t. We first observe that the point $(\xi,0,\mathbf{l})$ is a point belonging to the hypersurface of section $\mathscr{P}$ translated to the cell $\mathbf{l}$. As long as the time τ is between 0 and $T(\xi)$ the trajectory remains on the same segment attached to the position ξ and the cell $\mathbf{l}$. When $\tau=T(\xi)$, the trajectory performs its next passage through the hypersurface $\mathscr{P}$ at the point $\varphi(\xi)$. At this next passage, the trajectory may belong to a different cell $\mathbf{l}'$ of the lattice. We have therefore to introduce a function taking its values in the Bravais lattice $\mathbf{a}(\xi)\in\mathscr{L}$ which is the lattice vector of the jump between the cells $\mathbf{l}$ and $\mathbf{l}'$: $\mathbf{l}'-\mathbf{l}=\mathbf{a}(\xi)$.

At the next passage by the hypersurface of section, we have to identify the point $[\xi,T(\xi),\mathbf{l}]$ with the point $[\varphi(\xi),0,\mathbf{l}+\mathbf{a}(\xi)]$. In the special coordinates (8), we note that the flow is defined by the vector field $\mathbf{F}(\xi,\tau,\mathbf{l})=(0,1,0)$ [32]. The dynamics of the suspension flow is thus controlled by the mapping

$$\begin{aligned}\xi_{j+1}&=\varphi(\xi_j),\\ t_{j+1}&=t_j+T(\xi_j),\\ \mathbf{l}_{j+1}&=\mathbf{l}_j+\mathbf{a}(\xi_j),\end{aligned} \tag{9}$$

where $\{t_j\}_{j=-\infty}^{+\infty}$ are the successive times of passages through the hypersurface $\mathscr{P}$ and $\{\mathbf{l}_j\}_{j=-\infty}^{+\infty}$ the centers of the cells successively visited.

The time axis is divided into intervals of lengths $T(\varphi^j\xi)$ extending from $T(\xi)+\cdots+T(\varphi^{j-1}\xi)$ up to $T(\xi)+\cdots+T(\varphi^{j-1}\xi)+T(\varphi^j\xi)$ during which the position remains fixed at $\varphi^j\xi$ and the lattice vector at $\mathbf{l}+\mathbf{a}(\xi)+\cdots+\mathbf{a}(\varphi^{j-1}\xi)$. The flow is thus

$$\Phi^t(\xi,\tau,\mathbf{l})=(\xi,\tau+t,\mathbf{l}) \quad \text{for} \quad 0\leqslant\tau+t<T(\xi) \tag{10}$$

and

$$\Phi^t(\xi,\tau,\mathbf{l})=[\varphi^j\xi,\tau+t-T(\xi)-\cdots-T(\varphi^{j-1}\xi),\mathbf{l}+\mathbf{a}(\xi)+\cdots+\mathbf{a}(\varphi^{j-1}\xi)]$$
$$\text{for } 0\leqslant\tau+t-T(\xi)-\cdots-T(\varphi^{j-1}\xi)<T(\varphi^j\xi). \tag{11}$$

On the other hand, for the time running backward ($t<0$), we obtain

$$\Phi^{-|t|}(\xi,\tau,\mathbf{l})=[\varphi^{-j}\xi,\tau-|t|+T(\varphi^{-1}\xi)+\cdots+T(\varphi^{-j}\xi),\mathbf{l}-\mathbf{a}(\varphi^{-1}\xi)-\cdots-\mathbf{a}(\varphi^{-j}\xi)]$$
$$\text{for } 0\leqslant\tau-|t|+T(\varphi^{-1}\xi)+\cdots+T(\varphi^{-j}\xi)<T(\varphi^{-j}\xi). \tag{12}$$

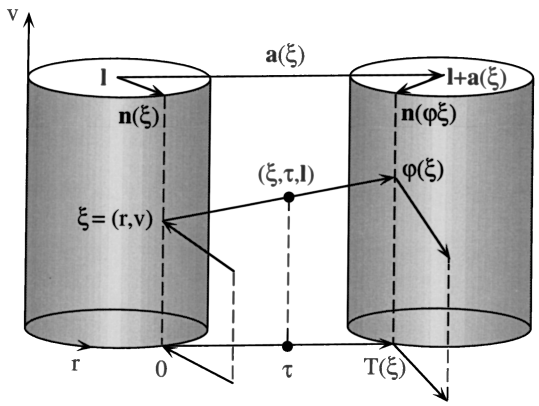

FIG. 1. Schematic representation of the suspension flow in the case of a planar billiard of the type of the Lorentz gas. The base of the cylinders is the two-dimensional position space available to the particle. The vertical axis of the cylinders corresponds to the projection of the velocity tangent to the walls at collisions. $\xi=(r,v)$ are the Birkhoff coordinates. $\varphi(\xi)$ is the image of the point ξ under the Birkhoff mapping. $\mathbf{l}$ is the center of the cell to which the point ξ is attached. $\mathbf{a}(\xi)$ is the jump vector so that $\mathbf{l}+\mathbf{a}(\xi)$ is the center of the cell to which the image $\varphi(\xi)$ is attached. $\mathbf{n}(\xi)$ and $\mathbf{n}(\varphi\xi)$ are the normal vectors from the centers of the cells to the points of collisions. $(\xi,\tau,\mathbf{l})$ are the coordinates of a current point of the flow with the time coordinate in $0\leqslant\tau<T(\xi)$.

In the following, we shall denote by $\phi^t(\xi,\tau)$ the flow in the elementary cell at the origin $\mathbf{l}=\mathbf{0}$. Thanks to the preceding definitions, we have carried out a reduction of the flow from the infinite phase space to a reduced flow in the fundamental domain obtained by using the translational symmetry on the lattice. This amounts to reducing the dynamics on the infinite plane to the dynamics on a torus by imposing periodic boundary conditions. We emphasize that the position of the particle in the infinite phase space can still be recovered from the lattice vector $\mathbf{l}$ together with the dynamics in the reduced phase space.

To establish the isomorphism between the coordinates of the suspension flow and the original coordinates of the system, we have to introduce the vector $\mathbf{n}(\xi)$ which gives the position of the point ξ of intersection with the hypersurface $\mathscr{P}$ with respect to the center $\mathbf{l}$ of the currently visited cell (see Fig. 1). At the instant of the intersection with $\mathscr{P}$, the position in the original coordinates is thus

$$\mathbf{r}(X)\big|_{\mathscr{P}}=\mathbf{r}(\xi,0,\mathbf{l})=\mathbf{l}+\mathbf{n}(\xi). \tag{13}$$

If we denote by $\mathbf{v}=\dot{\mathbf{r}}$ the velocity of the particle given by the first derivative of the position with respect to time we obtain the following relation for the segment of trajectory between the points $(\xi,0,\mathbf{l})$ and $[\varphi(\xi),0,\mathbf{l}+\mathbf{a}(\xi)]$:

$$\mathbf{a}(\xi)=\mathbf{n}(\xi)+\int_0^{T(\xi)}\mathbf{v}(\xi,\tau)d\tau-\mathbf{n}(\varphi\xi), \tag{14}$$

which is of importance for the following.

B. Assumption on the properties of the mapping

In order to develop the theory, we need to assume several properties for the suspension flow.

(I) The mapping φ is piecewise symplectic.

(II) The mapping φ is time-reversal symmetric.

(III) The mapping φ is hyperbolic in the sense that all the trajectories are unstable of saddle type with nonvanishing Lyapunov exponents. We also suppose that the mapping φ has the Kolmogorov property (K property) which implies ergodicity and mixing. Because of condition (I), ergodicity holds with respect to the Lebesgue measure ν in the coordinates ξ on $\mathscr{P}$. Moreover, the rate of mixing is assumed to be sufficiently fast for functions f and g which are piecewise Hölder continuous [33]. In our context, a stretched-exponential type of mixing may be supposed,

$$\left|\langle f(\varphi^j\xi)g(\xi)\rangle_\nu-\langle f\rangle_\nu\langle g\rangle_\nu\right|\leqslant\exp(-j^\gamma), \tag{15}$$

where $\langle\rangle_\nu$ denotes the average with respect to ν, j is large enough, and the constant γ is such that $0<\gamma<1$. This property of fast decay of correlations is known to imply the following central limit theorem [11], which we shall use later.

If f is piecewise Hölder continuous and $h=f-\langle f\rangle_\nu$, the following probability approaches the Gaussian error function asymptotically:

$$\lim_{n\to\infty}\nu\left\{\xi:\frac{1}{\sigma_h\sqrt{n}}\sum_{j=0}^{n-1}h(\varphi^j\xi)<y\right\}=\frac{1}{\sqrt{2\pi}}\int_{-\infty}^{y}\exp(-x^2/2)dx, \tag{16}$$

where the variance of fluctuations is given by the sum of the autocorrelation function of h,

$$\sigma_h^2=\sum_{j=-\infty}^{+\infty}\langle h(\xi)h(\varphi^j\xi)\rangle_\nu, \tag{17}$$

which is convergent according to (15).

Although condition (III) is essential, conditions (I) and (II) are not necessary for most of the following considerations which can be extended to dissipative systems and to one-dimensional maps as well.

Below, we discuss the consequences of conditions (I) and (II) and we define the general Frobenius-Perron operator. Thereafter, we describe the special case of billiards as examples of suspension flows.

C. Invariant measures

As a consequence of the piecewise symplectic property (I) of the mapping, we find

$$\left|\det\frac{\partial\varphi}{\partial\xi}\right|=1, \tag{18}$$

so that volumes are preserved in the Poincaré hypersurface of section $\mathscr{P}$. As aforementioned, the Lebesgue measure $\nu(d\xi)=d\xi$ is invariant under mapping φ. The average of a function $f(\xi)$ is defined by

$$\langle f\rangle_\nu=\frac{1}{|\mathscr{P}|}\int_{\mathscr{P}}f(\xi)d\xi, \tag{19}$$

where $|\mathscr{P}|=\int_{\mathscr{P}}d\xi$ is the volume of the hypersurface $\mathscr{P}$.

Consequently, we can define the corresponding invariant measures μ_∞ and μ of the flows Φ^t and ϕ^t, respectively, with the following averages of the quantity $F(X)$:

$$\langle F(X)\rangle_{\mu_\infty}=\int \mu_\infty(dX)F(X)=\sum_{\mathbf{l}\in\mathscr{L}}\int \mu(d\xi\, d\tau)F(\xi,\tau,\mathbf{l}), \tag{20}$$

where

$$\int \mu(d\xi\, d\tau)F(\xi,\tau,\mathbf{l})=\frac{1}{|\mathscr{P}|}\int_{\mathscr{P}}d\xi\int_0^{T(\xi)}\frac{d\tau}{\langle T\rangle_\nu}F(\xi,\tau,\mathbf{l}) =\frac{1}{\langle T\rangle_\nu}\left\langle\int_0^{T(\xi)}F(\xi,\tau,\mathbf{l})d\tau\right\rangle_\nu . \tag{21}$$

We denote by $\langle\rangle$ the average over the corresponding measure. The measure μ is equivalent to the Liouville measure describing the microcanonical ensemble in the energy shell $H=E$. The measure μ_∞ is not normalizable because it is defined on an infinite phase space. However, both the measures μ and ν are normalizable.

D. Time-reversal symmetry

The operation of time reversal is defined by the involution θ such that

$$\theta^2=1,$$
$$\theta\circ\varphi\circ\theta=\varphi^{-1},$$
$$T(\theta\xi)=T(\varphi^{-1}\xi),$$
$$\mathbf{a}(\theta\xi)=-\mathbf{a}(\varphi^{-1}\xi). \tag{22}$$

Under assumption (II), the suspension flow itself is time-reversal symmetric under the transformation

$$\Theta(\xi,\tau,\mathbf{l})=[\theta\circ\varphi(\xi),T(\xi)-\tau,\mathbf{l}+\mathbf{a}(\xi)] \quad \text{for } 0<\tau<T(\xi), \quad \text{such that } \Theta^2=1 \text{ and } \Theta\circ\Phi^t\circ\Theta=\Phi^{-t}. \tag{23}$$

This transformation corresponds to a reversal of the velocity of the particle. Since the trajectory is followed in the reversed direction, the lattice vector labeling the cell is also modified (cf. Fig. 1).

E. Liouvillian dynamics and the Frobenius-Perron operator

The phase-space dynamics induces a time evolution on the algebra of classical observables as well as on the probability densities representing nonequilibrium statistical ensembles, which is known as the Liouvillian dynamics. From these considerations, we can study the statistical mechanics of the system.

Let us consider an observable quantity $A(X)$ and the density $\rho(X)$ of some statistical ensemble defined on the infinite phase space (8) of the suspension flow. The statistical ensemble is arbitrary and may be considered as the initial ensemble of a time-evolution process. The average of the observables over the ensemble is given by

$$\langle A^*(X)\rho(X)\rangle_{\mu_\infty}=\int \mu_\infty(dX)A^*(X)\rho(X) =\sum_{\mathbf{l}\in\mathscr{L}}\int \mu(d\xi\, d\tau)A^*(\xi,\tau,\mathbf{l})\rho(\xi,\tau,\mathbf{l}). \tag{24}$$

The flow induces an evolution of this average according to

$$\langle A^*(\Phi^tX)\rho(X)\rangle_{\mu_\infty}=\langle A^*(X)\rho(\Phi^{-t}X)\rangle_{\mu_\infty} =\langle A^*(X)(\hat{P}^t\rho)(X)\rangle_{\mu_\infty}, \tag{25}$$

in which the Frobenius-Perron operator is defined as

$$\hat{P}^t\rho(X)=\rho(\Phi^{-t}X). \tag{26}$$

In the present work, the Frobenius-Perron operator is considered as a time-dependent bilinear functional taking its values on the complex numbers,

$$\{A|\hat{P}^t|\rho\}:\begin{pmatrix}A\in\mathscr{E}_A\\ \rho\in\mathscr{E}_\rho\end{pmatrix}\to\mathbb{C}, \tag{27}$$

in which both the observables A and the densities ρ belong to functional spaces $\mathscr{E}_A$ and $\mathscr{E}_\rho$ of smooth enough test functions.

F. Billiards as examples of suspension flows

As mentioned in the Introduction, billiards are special cases of suspension flows satisfying the preceding conditions, which we explicitly discuss in order to fix the ideas with a specific example.

Billiards are systems of hard particles in elastic collisions between themselves and with walls. Between the elastic collisions, the particles are free and their motion is described by the free Hamiltonian

$$H=\sum_{a=1}^{N}\frac{\mathbf{P}_a^2}{2M_a}=\frac{1}{2}\mathbf{v}^2, \tag{28}$$

where M_a are the masses of the particles and $\mathbf{P}_a=M_a\dot{\mathbf{R}}_a$ their momentum, and where the simplification follows from the change of coordinates $\mathbf{v}=\{\mathbf{P}_a/\sqrt{M_a}\}_{a=1}^N$ and $\mathbf{r}=\{\sqrt{M_a}\mathbf{R}_a\}_{a=1}^N$. If the particles are hard balls in a physical space of dimension f, the dimension of the position space is $F=Nf$. The flow Φ^t on the energy shell $H=E$ defines thus a phase space of dimension $D=2F-1$.

In position space, the billiard may be formed by a Bravais lattice $\mathscr{L}$ of obstacles which may be hard spheres or hard ellipsoids, for instance. Each collision on one of the obstacles is uniquely determined by the position and the velocity at the impact point in the hypersurface of the obstacles. These coordinates may be taken as the $D-1=2F-2$ canonically conjugate Birkhoff coordinates which are the $F-1$ positions in the hypersurface and the $F-1$ components of the velocity tangent to the hypersurface: $\xi=(\mathbf{r}_\perp,\mathbf{v}_\perp)$. The flow induces the so-called Birkhoff mapping φ which satisfies the above conditions (I) and (II) in these coordinates. The Birkhoff mapping may be hyperbolic

and ergodic under known conditions enunciated, in particular, by Bunimovich and Sinai [9]. The time-reversal operation is here defined by reversing the velocity at the collision: $\theta(\xi)=\theta(\mathbf{r}_\perp,\mathbf{v}_\perp)=(\mathbf{r}_\perp,-\mathbf{v}_\perp)$.

III. THE FROBENIUS-PERRON OPERATOR REDUCED BY SPATIAL TRANSLATIONS

In this section, we reduce the infinite system by using its symmetry under spatial translations. The observables and densities are reduced to functions defined in an elementary cell of the lattice thanks to Fourier transforms [14,28]. Thereafter, we construct the Frobenius-Perron operator acting on the spatial Fourier transforms.

A. Fourier transforms

We define a projection operator by

$$\hat{E}_{\mathbf{k}}=\sum_{\mathbf{l}\in\mathscr{L}}\exp(-i\mathbf{k}\cdot\mathbf{l})\hat{S}^{\mathbf{l}}, \tag{29}$$

in terms of the spatial translation operators

$$\hat{S}^{\mathbf{l}}f(\xi,\mathbf{l}')=f(\xi,\mathbf{l}+\mathbf{l}') \quad \text{for } \mathbf{l},\mathbf{l}'\in\mathscr{L}. \tag{30}$$

The projection operator (29) involves the so-called wave number $\mathbf{k}$. This latter is defined on the Brillouin zone $\mathscr{B}$ of the reciprocal lattice $\tilde{\mathscr{L}}$ [18]. The volume of the Brillouin zone is

$$|\mathscr{B}|=\int_{\mathscr{B}}d\mathbf{k}=\frac{(2\pi)^L}{|\det(\mathbf{l}_{10\ldots00},\ldots,\mathbf{l}_{00\ldots01}|}. \tag{31}$$

The operators (29) are projection operators since

$$\hat{E}_{\mathbf{k}}\hat{E}_{\mathbf{k}'}=|\mathscr{B}|\,\delta(\mathbf{k}-\mathbf{k}')\hat{E}_{\mathbf{k}}, \tag{32}$$

which is a consequence of the relation

$$\frac{1}{|\mathscr{B}|}\sum_{\mathbf{l}\in\mathscr{L}}\exp(i\mathbf{k}\cdot\mathbf{l})=\sum_{\mathbf{k}'\in\tilde{\mathscr{L}}}\delta(\mathbf{k}-\mathbf{k}'). \tag{33}$$

The identity operator is recovered by integrating the projection operator over the wave number

$$\hat{I}=\frac{1}{|\mathscr{B}|}\int_{\mathscr{B}}d\mathbf{k}\hat{E}_{\mathbf{k}}. \tag{34}$$

If ρ is a density defined on the infinite phase space, the function $\hat{E}_{\mathbf{k}}\rho$ is quasiperiodic on the lattice

$$\hat{E}_{\mathbf{k}}\rho(\xi,\tau,\mathbf{l})=\exp(i\mathbf{k}\cdot\mathbf{l})\hat{E}_{\mathbf{k}}\rho(\xi,\tau,0)=\exp(i\mathbf{k}\cdot\mathbf{l})\rho_{\mathbf{k}}(\xi,\tau). \tag{35}$$

The same relation holds for the Fourier components $A_{\mathbf{k}}(\xi,\tau)$ of an observable A. We have therefore a decomposition of each observable and each density over the infinite phase space into components defined in the reduced phase space and which depend continuously on the wave number $\mathbf{k}$.

The average (24) of the observable A over the density ρ can therefore be transformed into an integral over the Brillouin zone of an average over the reduced phase space

$$\langle A^*\rho\rangle_{\mu_\infty}=\frac{1}{|\mathscr{B}|}\int_{\mathscr{B}}d\mathbf{k}\langle A^*_{\mathbf{k}}\rho_{\mathbf{k}}\rangle_\mu. \tag{36}$$

The time evolution acts in a different way on each one of the components of the observables or densities as we shall show in the following section.

B. Frobenius-Perron operator for Fourier components

Our aim is to obtain the time evolution of the different components of the Fourier transform which is induced by the Frobenius-Perron operator (26). With this purpose, we consider the average of an observable A at time t that we decompose into a Fourier transform using the projection operators (29):

$$\langle A^*\hat{P}^t\rho\rangle_{\mu_\infty}=\langle A^*\rho^t\rangle_{\mu_\infty}=\frac{1}{|\mathscr{B}|}\int_{\mathscr{B}}d\mathbf{k}\langle A^*_{\mathbf{k}}\rho^t_{\mathbf{k}}\rangle_\mu, \tag{37}$$

where

$$\rho^t_{\mathbf{k}}(\xi,\tau)=\hat{E}_{\mathbf{k}}\hat{P}^t\rho(\xi,\tau,0). \tag{38}$$

Using Eq. (12), the action of the Frobenius-Perron operator on the density $\rho(X)$ is given by

$$\hat{P}^t\rho(\xi,\tau,0)=\rho[\Phi^{-t}(\xi,\tau,0)]=\rho[\varphi^{-j}\xi,\tau-t+T(\varphi^{-1}\xi)+\cdots+T(\varphi^{-j}\xi),-\mathbf{a}(\varphi^{-1}\xi)-\cdots-\mathbf{a}(\varphi^{-j}\xi)]$$

$$\text{for } 0\leqslant\tau-t+T(\varphi^{-1}\xi)+\cdots+T(\varphi^{-j}\xi)<T(\varphi^{-j}\xi). \tag{39}$$

Applying the projection operator $\hat{E}_{\mathbf{k}}$ and using the property of quasiperiodicity (35), we obtain

$$\hat{Q}^t_{\mathbf{k}}\rho_{\mathbf{k}}(\xi,\tau)\equiv\hat{E}_{\mathbf{k}}\hat{P}^t\rho(\xi,\tau,0)=\exp\{-i\mathbf{k}\cdot[\mathbf{a}(\varphi^{-1}\xi)+\cdots+\mathbf{a}(\varphi^{-j}\xi)]\}\rho_{\mathbf{k}}[\varphi^{-j}\xi,\tau-t+T(\varphi^{-1}\xi)+\cdots+T(\varphi^{-j}\xi)] \tag{40}$$

for t as in (39). Equation (40) defines a new Frobenius-Perron operator acting on the different Fourier components of the densities as

$$(\hat{Q}^t_{\mathbf{k}}F)(\xi,\tau)=\exp\{i\mathbf{k}\cdot\mathbf{l}[\Phi^{-t}(\xi,\tau,0)]\}F[\phi^{-t}(\xi,\tau)], \tag{41}$$

where the vector $\mathbf{l}[\Phi^t(\xi,\tau,0)]$ is the lattice vector corresponding to the path traveled by the point particle on the infinite phase space from the elementary cell at the origin up to the cell reached at the time t. According to Eqs. (10)–(12), this lattice vector is given by

$$\mathbf{l}[\Phi^t(\xi,\tau,0)]=\begin{cases}0 \quad \text{for } 0\leqslant\tau+t<T(\xi)\\ \mathbf{a}(\xi)+\cdots+\mathbf{a}(\varphi^{j-1}\xi) \quad \text{for } 0\leqslant\tau+t-T(\xi)-\cdots-T(\varphi^{j-1}\xi)<T(\varphi^j\xi),\end{cases} \tag{42}$$

and by

$$\mathbf{l}[\Phi^{-|t|}(\xi,\tau,0)]=-\mathbf{a}(\varphi^{-1}\xi)-\cdots-\mathbf{a}(\varphi^{-j}\xi)$$
$$\text{for } 0\leqslant\tau-|t|+T(\xi)+\cdots+T(\varphi^{-j}\xi)<T(\varphi^{-j}\xi). \tag{43}$$

We emphasize that the suspension flow is defined in such a way that the jumps between the lattice cells occur at the times $\{t_j\}$ of intersections with the hypersurface but not at intermediate times during the free flights between the successive passages. This construction introduces an important simplification in the following developments. We also point out that the Frobenius-Perron operator (41) explicitly depends on the wave number $\mathbf{k}$.

The time evolution of an average value is therefore decomposed like

$$\langle A^*\hat{P}^t\rho\rangle_{\mu_\infty}=\frac{1}{|\mathscr{B}|}\int_{\mathscr{B}}d\mathbf{k}\langle A^*_{\mathbf{k}}\hat{Q}^t_{\mathbf{k}}\rho_{\mathbf{k}}\rangle_\mu . \tag{44}$$

The Frobenius-Perron operator (41) has not been much studied until recently. When $\mathbf{k}=\mathbf{0}$, this Frobenius-Perron operator reduces to the usual one for the closed system in an elementary cell with periodic boundary conditions. Since the flow is assumed to be mixing, the spectrum of the operator $\hat{Q}^t_0$ considered in the Koopman approach admits $s=0$ for a unique discrete eigenvalue corresponding to the invariant probability measure (21) [34,35]. For $\mathbf{k}\neq\mathbf{0}$, the spectral properties are much less well known, although several recent works have been devoted to this problem, in particular, in the multibaker [13,15] but also in the Lorentz gas [28].

C. Time-reversal symmetry for Fourier components

The time-reversal transformation in phase space induces an operation on the observables and densities which is

$$(\hat{K}F)(X)=F^*(\Theta X), \tag{45}$$

and which has the effect that

$$\hat{K}\hat{P}^t\hat{K}=\hat{P}^{-t}. \tag{46}$$

At the level of the spatial Fourier transform, this operation reverses the wave number as expected,

$$\hat{K}\hat{E}_{\mathbf{k}}=\hat{E}_{-\mathbf{k}}\hat{K}. \tag{47}$$

Hence the Frobenius-Perron operator of the $\mathbf{k}$ component is transformed according to

$$\hat{K}\hat{Q}^t_{\mathbf{k}}=\hat{Q}^{-t}_{-\mathbf{k}}\hat{K}. \tag{48}$$

Using these symmetry properties, we obtain the relations

$$\langle(\hat{K}A)^*_{\mathbf{k}}\hat{Q}^t_{\mathbf{k}}(\hat{K}\rho)_{\mathbf{k}}\rangle^*_\mu=\langle A^*_{-\mathbf{k}}\hat{Q}^{-t}_{-\mathbf{k}}\rho_{-\mathbf{k}}\rangle_\mu$$
$$=\langle\rho_{-\mathbf{k}}(\hat{Q}^t_{-\mathbf{k}}A_{-\mathbf{k}})^*\rangle_\mu , \tag{49}$$

which show how the forward and backward semigroups in the sectors with the wave numbers $\mathbf{k}$ and $-\mathbf{k}$ are interrelated.

IV. THE SPECIAL FROBENIUS-PERRON OPERATOR OF THE SUSPENSION FLOW

A. From the flow to the mapping

Pollicott has shown how the Frobenius-Perron operator of a suspension flow can be simplified [5]. We are interested by the analytic continuation of the time Fourier transforms of correlation functions such as

$$\tilde{C}_{AB}(\omega)=\int_{-\infty}^{+\infty}dt\ \exp(i\omega t)\langle A(\Phi^tX)B(X)\rangle_\mu , \tag{50}$$

assuming that $\langle A\rangle_\mu=\langle B\rangle_\mu=0$. In the presence of decay processes, it is necessary to split the Fourier transform over the whole time axis into two semisided Fourier transforms for positive and negative times, in which case analytic continuation amounts to considering Laplace transforms (with $\omega=is$). The Laplace transform for positive times defines the forward semigroup while the one for negative times defines the backward semigroup.

Because the time evolution of a suspension flow is piecewise defined according to Eqs. (10)–(12) and (41)–(43), the integral over the time can be transformed into a sum of integrals over the evolution between the intersections in the hypersurface of section as

$$\int_0^\infty dt\ \exp(-st)\hat{Q}^t_{\mathbf{k}}F(\xi,\tau)=\int_0^\tau dt\ \exp(-st)F(\xi,\tau-t)+\sum_{n=1}^{\infty}\int_{\tau+T(\varphi^{-1}\xi)+\cdots+T(\varphi^{-n}\xi)}^{\tau+T(\varphi^{-1}\xi)+\cdots+T(\varphi^{-n+1}\xi)}dt\ \exp(-st)$$
$$\times\exp\left[-i\mathbf{k}\cdot\sum_{j=1}^{n}\mathbf{a}(\varphi^{-j}\xi)\right]F\left[\varphi^{-n}\xi,\tau-t+\sum_{j=1}^{n}T(\varphi^{-j}\xi)\right], \tag{51}$$

for $\mathrm{Re}s>0$. Performing changes of variables, the Laplace transform is written

$$\int_0^\infty dt\ \exp(-st)\hat{Q}_{\mathbf{k}}^t F(\xi,\tau)=\exp(-s\tau)\int_0^\tau d\tau'\exp(s\tau')F(\xi,\tau')+\sum_{n=1}^\infty \exp(-s\tau)$$
$$\times\exp\left[-s\sum_{j=1}^n T(\varphi^{-j}\xi)-i\mathbf{k}\cdot\sum_{j=1}^n \mathbf{a}(\varphi^{-j}\xi)\right]\int_0^{T(\varphi^{-n}\xi)} d\tau'\exp(s\tau')F(\varphi^{-n}\xi,\tau'). \quad (52)$$

Equation (52) becomes

$$\int_0^\infty dt\ \exp(-st)\hat{Q}_{\mathbf{k}}^t F(\xi,\tau)=\exp(-s\tau)\left[\int_0^\tau d\tau'\exp(s\tau')F(\xi,\tau')+\sum_{n=1}^\infty \hat{R}_{\mathbf{k},s}^n f_s(\xi)\right], \quad (53)$$

if we introduce the function

$$f_s(\xi)=\int_0^{T(\xi)} d\tau'\exp(s\tau')F(\xi,\tau') \quad (54)$$

and the following Frobenius-Perron operator of the mapping φ:

$$(\hat{R}_{\mathbf{k},s}f)(\xi)=\exp[-sT(\varphi^{-1}\xi)-i\mathbf{k}\cdot\mathbf{a}(\varphi^{-1}\xi)]f(\varphi^{-1}\xi). \quad (55)$$

This new Frobenius-Perron operator depends not only on the wave number $\mathbf{k}$ but also on the complex variable s which will give the relaxation rate of the system. For $\mathbf{k}=\mathbf{0}$, we recover the Frobenius-Perron operator previously introduced by Pollicott for suspension flows. When the calculation is carried out for the Fourier transform over the whole time axis as performed by Pollicott [5], there is no extra term as for Eq. (53), in which the initial time may fall between two successive collisions.

The adjoint of the Frobenius-Perron operator (55) is defined by requiring that

$$\langle g^*(\hat{R}_{\mathbf{k},s}f)\rangle_\nu=\langle(\hat{R}_{\mathbf{k},s}^\dagger g)^* f\rangle_\nu, \quad (56)$$

so that

$$(\hat{R}_{\mathbf{k},s}^\dagger g)(\xi)=\exp[-s^*T(\xi)+i\mathbf{k}\cdot\mathbf{a}(\xi)]g(\varphi\xi). \quad (57)$$

B. Eigenvalue problem and ζ function

If we consider the Frobenius-Perron operator (55) as a transfer operator acting on smooth test functions, we can pose an eigenvalue problem as follows. Eigenvalues are defined as the zeros of the complex variable s of the Fredholm determinant [6]

$$\mathrm{Det}(\hat{I}-\hat{R}_{\mathbf{k},s})=0. \quad (58)$$

If such zeros exist, they depend parametrically on the wave number $\mathbf{k}$. The work of Cvitanović and co-workers [36] has shown that the zeros may be obtained in terms of periodic orbits. The Fredholm determinant (58) is given as a Selberg-Smale ζ function which is itself a product of inverse Ruelle ζ functions [6,28]:

$$\mathrm{Det}(\hat{I}-\hat{R}_{\mathbf{k},s})=\prod_p\prod_{m_1,\ldots,m_u=0}\left[1-\frac{\exp(-sT_p-i\mathbf{k}\cdot\mathbf{a}_p)}{|\Lambda_p^{(1)}\cdots\Lambda_p^{(u)}|\Lambda_p^{(1)m_1}\cdots\Lambda_p^{(u)m_u}}\right]^{(m_1+1)\cdots(m_u+1)}\equiv Z(s;\mathbf{k}), \quad (59)$$

where we assumed that all the periodic orbits are of hyperbolic type in each of the directions transverse to the flow and that the stability eigenvalues of the linearized Poincaré section transverse to the orbit come in pairs $\{\Lambda_p^{(i)},\Lambda_p^{(i)-1}\}_{i=1}^u$ with $u=(D-1)/2$. The first product extends over all the prime periodic orbits p of the mapping φ. The second product runs over the integers $m_1,\ldots,m_u$. The vector $\mathbf{a}_p$ gives the distance traveled by the particle on the lattice during the prime period T_p of p. If n_p is the number of collisions during the prime period of p and if ξ_p is some initial condition, these quantities are given by, respectively,

$$T_p=\sum_{j=0}^{n_p-1} T(\varphi^j\xi_p),\quad \mathbf{a}_p=\sum_{j=0}^{n_p-1}\mathbf{a}(\varphi^j\xi),\quad \det\left[\frac{\partial\varphi^{n_p}}{\partial\xi}(\xi_p)-\Lambda\mathbf{l}\right]=0. \quad (60)$$

In the present context of suspension flows, the result (59) can be derived as follows:

$$\mathrm{Det}(\hat{I}-\hat{R}_{\mathbf{k},s})=\exp\ \ln\ \mathrm{Det}(\hat{I}-\hat{R}_{\mathbf{k},s})=\exp\ \mathrm{Tr}\ \ln(\hat{I}-\hat{R}_{\mathbf{k},s})=\exp\left(-\sum_{n=1}^\infty\frac{1}{n}\mathrm{Tr}\hat{R}_{\mathbf{k},s}^n\right), \quad (61)$$

with the trace defined by

$$\mathrm{Tr}\hat{R}^n_{\mathbf{k},s}=\int_{\mathscr{P}}\left\{\exp\sum_{j=1}^{n}\left[-sT(\varphi^{-j}\xi)-i\mathbf{k}\cdot\mathbf{a}(\varphi^{-j}\xi)\right]\right\}\delta(\xi-\varphi^n\xi)d\xi. \tag{62}$$

The kernel of the Frobenius-Perron operator is given by a Dirac distribution which can be decomposed as follows:

$$\delta(\xi-\varphi^n\xi)=\sum_{\tilde{\xi}=\varphi^n\tilde{\xi}}\frac{\delta(\xi-\tilde{\xi})}{|\det[\mathbf{l}-\partial_\xi\varphi^n(\tilde{\xi})]|}. \tag{63}$$

With the previous assumption on the stability eigenvalues, the determinant in the denominator of (63) can be written as

$$|\det[\mathbf{l}-\partial_\xi\varphi^{rn_p}(\tilde{\xi})]|^{-1}=\prod_{i=1}^{u}|\Lambda_p^{(i)r}|^{-1}\left(1-\frac{1}{\Lambda_p^{(i)r}}\right)^{-2}=\sum_{m_1,\ldots,m_u=0}^{\infty}\frac{(m_1+1)\cdots(m_u+1)}{[|\Lambda_p^{(1)}\cdots\Lambda_p^{(u)}|\Lambda_p^{(1)m_1}\cdots\Lambda_p^{(u)m_u}]^r}, \tag{64}$$

where we supposed that the fixed point $\tilde{\xi}$ of φ^n belongs to a periodic orbit of prime period n_p which is repeated r times during the $n=rn_p$ iterations. The sum over the n iterations and over the fixed points $\tilde{\xi}$ can be transformed into a sum over the prime periodic orbits and their repetitions according to $\Sigma_{n=1}^{\infty}\Sigma_{\tilde{\xi}=\varphi^n\tilde{\xi}}=\Sigma_{r=1}^{\infty}\Sigma_p n_p$. The sum over the repetition number can be performed and the Taylor expansion $\ln(1-y)=-\Sigma_{r=1}^{\infty}(y^r/r)$ used again to finally obtain the Selberg-Smale ζ function (59) with the characteristic quantities (60) for the periodic orbits. Q.E.D.

Let us now describe a few properties of the ζ function. For the forward semigroup, no zero is expected when Res is positive and large enough. The zeros are expected for analytic continuation toward negative values of Res. Several kinds of singularities, such as simple zeros, multiple zeros, or branch cuts, may be encountered. When the wave number vanishes, $\mathbf{k}=\mathbf{0}$, the ζ function admits a simple zero at $s=0$ because the system is mixing. This zero corresponds to the ergodic invariant probability measure given by (19) which has a uniform density function: $\psi_0(\xi)=1$. Here, we are interested in the behavior of this zero when the wave number is tuned away from $\mathbf{k}=\mathbf{0}$. We may expect that for $\mathbf{k}$ small enough, there exists a zero $s=s_{\mathbf{k}}$ and a corresponding eigenstate $\psi_{\mathbf{k}}(\xi)$ such that

$$\hat{R}_{\mathbf{k},s_{\mathbf{k}}}\psi_{\mathbf{k}}(\xi)=\psi_{\mathbf{k}}(\xi). \tag{65}$$

When $\mathbf{k}\neq\mathbf{0}$, we no longer expect that the eigenstate $\psi_{\mathbf{k}}$ is a function. Works on the multibaker suggest that the eigenstate is a distribution which acquires a meaning only when it is applied to a smooth enough test function $g(\xi)$ such that $\langle g^*\psi_{\mathbf{k}}\rangle$ becomes a well-defined complex number. This result has been proved for the multibaker [15,16]. Here, we assume that the eigenvalue $s_{\mathbf{k}}$ and the eigendistribution $\psi_{\mathbf{k}}$ can be differentiated N times at small enough wave numbers $\mathbf{k}$, with N large enough and possibly arbitrarily large. According to this assumption, we carry out successive differentiations of the eigenvalue equation (65) to obtain the nonequilibrium steady state, the diffusion coefficient given by the Green-Kubo relation, Fick's law, as well as the higher-order diffusion coefficients [37–39]. It will become clear in the following that the derivatives of the eigenstate $\psi_{\mathbf{k}}$ at $\mathbf{k}=\mathbf{0}$ are distributions (singular measures).

Assuming the existence of the eigenstate in (65), the adjoint (57) of the Frobenius-Perron operator also admits an eigenstate

$$\hat{R}^{\dagger}_{\mathbf{k},s_{\mathbf{k}}}\tilde{\psi}_{\mathbf{k}}(\xi)=\tilde{\psi}_{\mathbf{k}}(\xi), \tag{66}$$

which plays the role of the left eigenstate of the Frobenius-Perron operator itself while $\psi_{\mathbf{k}}$ is the right eigenstate. We may also assume that both eigenstates satisfy the normalization condition

$$\langle\tilde{\psi}^*_{\mathbf{k}}\psi_{\mathbf{k}}\rangle_\nu=1. \tag{67}$$

C. Consequences of time-reversal symmetry

Time-reversal symmetry has important consequences on the eigenvalues of the Frobenius-Perron operator, which can be deduced thanks to the ζ function (59). To each periodic orbit p, a time-reversed periodic orbit θp is associated such that

$$T_{\theta p}=T_p,\quad \mathbf{a}_{\theta p}=-\mathbf{a}_p,\quad \Lambda^{(i)}_{\theta p}=\Lambda^{(i)}_p\quad (i=1,\ldots,u). \tag{68}$$

Moreover, we note that all these characteristic quantities are real. Equation (68) therefore implies that the product over periodic orbits in the ζ function $Z(s_{\mathbf{k}};\mathbf{k})=0$ can be rewritten to get $Z(s_{\mathbf{k}};-\mathbf{k})=0$. On the other hand, taking the complex conjugate of the ζ function implies that $Z(s^*_{\mathbf{k}};-\mathbf{k})=0$. Therefore the eigenvalues satisfy the relations

$$s_{\mathbf{k}}=s_{-\mathbf{k}}\quad\text{and}\quad s^*_{\mathbf{k}}=s^*_{-\mathbf{k}}. \tag{69}$$

These relations can also be obtained from Eq. (49).

Introducing the operator

$$\hat{\kappa}f(\xi)=f^*(\theta\xi),\ \text{such that}\ \hat{\kappa}^2=\hat{I}, \tag{70}$$

the Frobenius-Perron operator of the mapping is related to its adjoint by

$$\hat{\kappa}\hat{R}_{\mathbf{k},s}\hat{\kappa}=\hat{R}^{\dagger}_{-\mathbf{k},s}. \tag{71}$$

Therefore the time-reversal symmetry implies that the left and right eigenstates are related by

$$\tilde{\psi}_{\mathbf{k}}(\xi) = \psi^*_{-\mathbf{k}}(\theta\xi). \tag{72}$$

As we mentioned in the Introduction, if the right eigenstates are smooth along the unstable directions, the left eigenstates are smooth along the stable directions because the stable and unstable directions are exchanged by the time-reversal transformation θ.

D. Relation to the eigenvalue problem for the flow

Since the original problem concerns the flow and the Frobenius-Perron operator (41), we need to establish the connection between the eigenstate (65) and the eigenstate corresponding to the flow, namely,

$$(\hat{Q}^t_{\mathbf{k}}\Psi_{\mathbf{k}})(\xi,\tau) = \exp(s_{\mathbf{k}}t)\Psi_{\mathbf{k}}(\xi,\tau). \tag{73}$$

If we take the Laplace transform of both members of Eq. (73) and if we use Eq. (53) introducing the transform (54) of the eigenstate as

$$\Upsilon_{\mathbf{k},s}(\xi) = \int_0^{T(\xi)} d\tau' \exp(s\tau')\Psi_{\mathbf{k}}(\xi,\tau'), \tag{74}$$

the eigenvalue equation becomes

$$\int_0^{\tau} d\tau' \exp(s\tau')\Psi_{\mathbf{k}}(\xi,\tau') + \sum_{n=1}^{\infty} \hat{R}^n_{\mathbf{k},s}\Upsilon_{\mathbf{k},s}(\xi) = \frac{\exp(s\tau)}{s-s_{\mathbf{k}}}\Psi_{\mathbf{k}}(\xi,\tau) \tag{75}$$

for $0 \leqslant \tau < T(\xi)$.

Using the relation

$$\sum_{n=1}^{\infty} \hat{R}^n_{\mathbf{k},s} = \frac{\hat{R}_{\mathbf{k},s}}{\hat{I}-\hat{R}_{\mathbf{k},s}}, \tag{76}$$

and setting $\tau = 0$, we obtain

$$(\hat{I}-\hat{R}_{\mathbf{k},s})\Psi_{\mathbf{k}}(\xi,0) = (s-s_{\mathbf{k}})\hat{R}_{\mathbf{k},s}\Upsilon_{\mathbf{k},s}(\xi). \tag{77}$$

The equality $s = s_{\mathbf{k}}$ leads to

$$(\hat{I}-\hat{R}_{\mathbf{k},s_{\mathbf{k}}})\Psi_{\mathbf{k}}(\xi,0) = 0, \tag{78}$$

which shows that the eigenstate of the flow at $\tau = 0$ may be identified with the eigenstate of the mapping defined by (65),

$$\Psi_{\mathbf{k}}(\xi,0) = \psi_{\mathbf{k}}(\xi). \tag{79}$$

To determine the eigenstate of the flow for the other values of τ, we differentiate Eq. (75) with respect to τ to get

$$\partial_\tau \Psi_{\mathbf{k}}(\xi,\tau) = -s_{\mathbf{k}}\Psi_{\mathbf{k}}(\xi,\tau), \tag{80}$$

whose solution is

$$\Psi_{\mathbf{k}}(\xi,\tau) = \exp(-s_{\mathbf{k}}\tau)\psi_{\mathbf{k}}(\xi) \quad \text{for } 0 \leqslant \tau < T(\xi). \tag{81}$$

We emphasize that Eq. (81) holds for $\tau < T(\xi)$. At $\tau = T(\xi)$, the distribution $\Psi_{\mathbf{k}}$ acquires a phase due to the jump in the lattice vector according to

$$\Psi_{\mathbf{k}}[\xi, T(\xi)] = \exp[i\mathbf{k}\cdot\mathbf{a}(\xi)]\Psi_{\mathbf{k}}(\varphi\xi,0), \tag{82}$$

in agreement with the eigenvalue equation (65). We also notice that, since $s_{\mathbf{k}} < 0$, the eigenstate (81) presents an exponential growth which only lasts for a finite time interval after which the exponential damping expected from Eq. (73) prevails. In this way, the eigenvalue problem formulated at the level of the flow and of the mapping are interconnected.

V. FROM THE EIGENSTATES TO THE NONEQUILIBRIUM STEADY STATES

In this section, we construct the nonequilibrium steady state starting from Eqs. (65)–(67) defining the left and right eigenvectors. We perform successive differentiations of these equations with respect to the wave number. The resulting expressions are thereafter evaluated for a vanishing wave number.

A. Mean drift

Differentiating the normalization condition (67) with respect to the wave number, we obtain

$$\langle \partial_{\mathbf{k}}\tilde{\psi}^*_{\mathbf{k}}\psi_{\mathbf{k}}\rangle_\nu + \langle \tilde{\psi}^*_{\mathbf{k}}\partial_{\mathbf{k}}\psi_{\mathbf{k}}\rangle_\nu = 0. \tag{83}$$

On the other hand, the normalization condition can be rewritten using the eigenvalue equation as

$$\langle \tilde{\psi}^*_{\mathbf{k}}\psi_{\mathbf{k}}\rangle_\nu = \langle \tilde{\psi}^*_{\mathbf{k}}\hat{R}_{\mathbf{k},s_{\mathbf{k}}}\psi_{\mathbf{k}}\rangle_\nu = 1, \tag{84}$$

which is also differentiated with respect to the wave number, to get

$$\langle \partial_{\mathbf{k}}\tilde{\psi}^*_{\mathbf{k}}\hat{R}_{\mathbf{k},s_{\mathbf{k}}}\psi_{\mathbf{k}}\rangle_\nu + \langle \tilde{\psi}^*_{\mathbf{k}}\hat{R}_{\mathbf{k},s_{\mathbf{k}}}\partial_{\mathbf{k}}\psi_{\mathbf{k}}\rangle_\nu + \langle \tilde{\psi}^*_{\mathbf{k}}[-\partial_{\mathbf{k}}s_{\mathbf{k}}T(\varphi^{-1}\xi) - i\mathbf{a}(\varphi^{-1}\xi)]\hat{R}_{\mathbf{k},s_{\mathbf{k}}}\psi_{\mathbf{k}}\rangle_\nu = 0. \tag{85}$$

The eigenvalue equation (65) and Eqs. (83) and (84) yield

$$-\partial_{k_\alpha}s_{\mathbf{k}}\langle \tilde{\psi}^*_{\mathbf{k}}T(\varphi^{-1}\xi)\psi_{\mathbf{k}}\rangle_\nu - i\langle \tilde{\psi}^*_{\mathbf{k}}a_\alpha(\varphi^{-1}\xi)\psi_{\mathbf{k}}\rangle_\nu = 0 \tag{86}$$

or

$$\partial_{\mathbf{k}}s_{\mathbf{k}} = -i\frac{\langle \tilde{\psi}^*_{\mathbf{k}}\mathbf{a}(\varphi^{-1}\xi)\psi_{\mathbf{k}}\rangle_\nu}{\langle \tilde{\psi}^*_{\mathbf{k}}T(\varphi^{-1}\xi)\psi_{\mathbf{k}}\rangle_\nu}. \tag{87}$$

In the limit $\mathbf{k} = \mathbf{0}$, the mean drift is vanishing,

$$\partial_{\mathbf{k}}s_0 = 0, \tag{88}$$

because $\psi_0 = \psi^*_0 = 1$ and $\langle \mathbf{a}(\xi)\rangle_\nu = 0$.

B. The first derivative of the eigenstate with respect to the wave number

As mentioned in the Introduction, the nonequilibrium steady state corresponding to a constant concentration gradient across the system is given by the derivative of the eigenstate with respect to the wave number and evaluated at

$\mathbf{k}=\mathbf{0}$ [cf. Eq. (5)]. In order to get the derivative of the eigenstate, we differentiate the eigenvalue equation (65) directly with respect to $\mathbf{k}$ to obtain

$$[-\partial_{\mathbf{k}}s_{\mathbf{k}}T(\varphi^{-1}\xi)-i\mathbf{a}(\varphi^{-1}\xi)](\hat{R}_{\mathbf{k},s_{\mathbf{k}}}\psi_{\mathbf{k}})(\xi)+(\hat{R}_{\mathbf{k},s_{\mathbf{k}}}\partial_{\mathbf{k}}\psi_{\mathbf{k}})(\xi) = \partial_{\mathbf{k}}\psi_{\mathbf{k}}(\xi). \quad (89)$$

At $\mathbf{k}=\mathbf{0}$, the first derivative of the eigenvalue vanishes because of (88) while the eigenstate becomes the microcanonical measure: $\psi_0=1$. Therefore the gradient state obeys the functional equation

$$\partial_{\mathbf{k}}\psi_0(\varphi^{-1}\xi)-i\mathbf{a}(\varphi^{-1}\xi)=\partial_{\mathbf{k}}\psi_0(\xi), \quad (90)$$

which is one of our main results.

Similarly, the differentiation of the adjoint eigenvalue equation (66) leads to

$$\partial_{\mathbf{k}}\tilde{\psi}_0(\varphi\xi)+i\mathbf{a}(\xi)=\partial_{\mathbf{k}}\tilde{\psi}_0(\xi). \quad (91)$$

Equations (90) and (91) admit the solutions

$$\partial_{\mathbf{k}}\psi_0(\xi)=-i\sum_{j=1}^{\infty}\mathbf{a}(\varphi^{-j}\xi), \quad (92)$$

$$\partial_{\mathbf{k}}\tilde{\psi}_0(\xi)=+i\sum_{j=0}^{\infty}\mathbf{a}(\varphi^{j}\xi), \quad (93)$$

as can be checked directly. Nevertheless, we notice that the solutions for the gradients of the left and right eigenstates can be exchanged. In order to resolve this ambiguity, we need to go back to the condition of forward semigroup. The eigenstate $\psi_{\mathbf{k}}$ is obtained by successive applications of the forward evolution operator. It corresponds to a density which is propagated in the future. Now, we observe that the forward propagation involves the inverse mapping φ^{-1} as shown by (55) while the backward propagation involves the direct mapping φ. Therefore the solution of (90) which is consistent with the forward propagation must be taken as (92) and not as (93). In this way, the ambiguity is resolved.

C. Nonequilibrium steady states

According to Eq. (5), the nonequilibrium steady state corresponding to a gradient of concentration in the direction of the constant vector $\mathbf{g}$ is given by [30,31]

$$\psi_{\mathbf{g}}(\xi)=-i\mathbf{g}\cdot\partial_{\mathbf{k}}\psi_0(\xi)=-\sum_{j=1}^{\infty}\mathbf{g}\cdot\mathbf{a}(\varphi^{-j}\xi). \quad (94)$$

Considered as a function, $\psi_{\mathbf{g}}$ is meaningless. However, the assumed property of decay of correlations (15) gives a meaning to (94) in the sense of a distribution acting on test functions $f(\xi)$ which are piecewise Hölder continuous. Indeed, if $f(\xi)$ is such a function we have that

$$|\langle f(\xi)\mathbf{g}\cdot\mathbf{a}(\varphi^{-j}\xi)\rangle_{\nu}|\leqslant\exp(-j^{\gamma}) \quad (95)$$

for j large enough, since $\mathbf{g}\cdot\mathbf{a}(\xi)$ is also a piecewise Hölder continuous function of vanishing mean value. As a consequence, the sum

$$\langle f(\xi)\psi_{\mathbf{g}}(\xi)\rangle_{\nu}=-\sum_{j=1}^{\infty}\langle f(\xi)\mathbf{g}\cdot\mathbf{a}(\varphi^{-j}\xi)\rangle_{\nu} \quad (96)$$

is convergent and $\langle f(\xi)\psi_{\mathbf{g}}(\xi)\rangle_{\nu}$ is therefore a finite number. A similar reasoning shows that both (92) and (93) are also linear functionals known as distributions.

The distribution (96) may be considered as a nonpositive measure which is singular with respect to the Lebesgue measure because its kernel $\psi_{\mathbf{g}}(\xi)$ is not a function as shown by the following property.

According to the central limit theorem (16), the probability for the sum (94) to remain in the finite interval $[-\eta,+\eta]$ is equal to

$$\nu\left\{\xi:-\eta<\sum_{j=1}^{n}\mathbf{g}\cdot\mathbf{a}(\varphi^{-j}\xi)<+\eta\right\}\underset{n\to\infty}{\simeq}\frac{2\eta}{\sigma_{\mathbf{g}\cdot\mathbf{a}}\sqrt{2\pi n}}. \quad (97)$$

Since this probability vanishes in the limit $n\to\infty$ we may expect that the sum remains finite only on a set of zero Lebesgue measure. In Sec. VII, we shall see that the distribution (94) defining the nonequilibrium steady state may be represented by its cumulative function, in the particular case of the Lorentz gas.

With respect to the flow dynamics, the nonequilibrium steady state can be obtained using Eq. (81) as

$$\Psi_{\mathbf{g}}(\xi,\tau)=-i\mathbf{g}\cdot\partial_{\mathbf{k}}\Psi_0(\xi,\tau)=\psi_{\mathbf{g}}(\xi)\ \text{ for }\ 0\leqslant\tau<T(\xi). \quad (98)$$

Since the eigenstate $\Psi_{\mathbf{k}}$ is quasiperiodic over the lattice, i.e., that

$$\Psi_{\mathbf{k}}(\xi,\tau,\mathbf{l})=\exp(i\mathbf{k}\cdot\mathbf{l})\Psi_{\mathbf{k}}(\xi,\tau,0), \quad (99)$$

the nonequilibrium steady state satisfies

$$\Psi_{\mathbf{g}}(\xi,\tau,\mathbf{l})=\mathbf{g}\cdot\mathbf{l}+\Psi_{\mathbf{g}}(\xi,\tau,0)=\mathbf{g}\cdot\mathbf{l}+\psi_{\mathbf{g}}(\xi) =\mathbf{g}\cdot\mathbf{l}-\sum_{j=1}^{\infty}\mathbf{g}\cdot\mathbf{a}(\varphi^{-j}\xi), \quad (100)$$

which shows that the measure increases linearly in the direction of the gradient as expected from (5). However, we observe that the exact deterministic construction involves a new term with respect to (5), which describes fluctuations around the nonequilibrium steady state.

A time-reversed nonequilibrium steady state can also be defined from the adjoint eigenstate $\tilde{\psi}_{\mathbf{k}}$ as

$$\tilde{\psi}_{\mathbf{g}}(\xi,\tau,\mathbf{l})=\mathbf{g}\cdot\mathbf{l}+\tilde{\psi}_{\mathbf{g}}(\xi)=\mathbf{g}\cdot\mathbf{l}+\sum_{j=0}^{\infty}\mathbf{g}\cdot\mathbf{a}(\varphi^{j}\xi). \quad (101)$$

Using Eqs. (13) and (14), we notice that the distribution corresponding to a constant gradient of concentration is simply given by

$$\Psi_{\mathbf{g}}(X)=\mathbf{g}\cdot\mathbf{r}(X)+\int_{0}^{-\infty}\mathbf{g}\cdot\mathbf{v}(\Phi^{t}X)dt, \quad (102)$$

where $\mathbf{v}(\Phi^t X)$ is the velocity at time t of the trajectory from the initial condition X. Similarly, the time-reversed nonequilibrium steady state is

$$\tilde{\Psi}_{\mathbf{g}}(X)=\mathbf{g}\cdot\mathbf{r}(X)+\int_0^{+\infty}\mathbf{g}\cdot\mathbf{v}(\Phi^t X)dt. \tag{103}$$

Equations (102) and (103)—which constitute the central result of the present work—give the nonequilibrium steady states in terms of the continuous-time flow without reference to the mapping. We may thus conclude that Eqs. (102) and (103) are general expressions, which apply to general Hamiltonian flows in the sense of distributions. As a corollary, the singular character of the nonequilibrium states also appears as a general result.

In contrast with the scaling theories of diffusion, the nonequilibrium steady states are here defined at the microscopic level of phase space. In this regard, such nonequilibrium measures naturally generalize the equilibrium measures. A crucial aspect is that the support of the nonequilibrium measures we consider here is the plain phase space of integer dimension $D-1$ in the space $\mathscr{P}$ of ξ. This is a difference with respect to the chaotic-scattering approach concerned with open systems where the support of the invariant measure is fractal. Nevertheless, the present measures remain singular and are therefore different from the measure of the microcanonical ensemble, which is the Sinai-Bowen-Ruelle measure associated with the mapping φ.

It will be checked here below that the nonequilibrium steady states obey Fick's law. Before reaching this result, we need to determine the diffusion matrix.

D. Diffusion matrix

Differentiating Eq. (86) again with respect to the wave number, we get

$$-\partial_{k_\alpha}\partial_{k_\beta}s_{\mathbf{k}}\langle\tilde{\psi}^*_{\mathbf{k}}T(\varphi^{-1}\xi)\psi_{\mathbf{k}}\rangle_\nu-\partial_{k_\alpha}s_{\mathbf{k}}\langle\partial_{k_\beta}\tilde{\psi}^*_{\mathbf{k}}T(\varphi^{-1}\xi)\psi_{\mathbf{k}}\rangle_\nu-\partial_{k_\alpha}s_{\mathbf{k}}\langle\tilde{\psi}^*_{\mathbf{k}}T(\varphi^{-1}\xi)\partial_{k_\beta}\psi_{\mathbf{k}}\rangle_\nu-i\langle\partial_{k_\beta}\tilde{\psi}^*_{\mathbf{k}}a_\alpha(\varphi^{-1}\xi)\psi_{\mathbf{k}}\rangle_\nu$$
$$-i\langle\tilde{\psi}^*_{\mathbf{k}}a_\alpha(\varphi^{-1}\xi)\partial_{k_\beta}\psi_{\mathbf{k}}\rangle_\nu=0 \tag{104}$$

for $\alpha,\beta=1,\ldots,L$. Taking the limit $\mathbf{k}=\mathbf{0}$, using Eq. (88), and $\psi_0=\tilde{\psi}_0=1$, we obtain

$$\partial_{k_\alpha}\partial_{k_\beta}s_0=-\frac{i}{\langle T\rangle_\nu}[\langle\partial_{k_\beta}\tilde{\psi}^*_0 a_\alpha(\varphi^{-1}\xi)\rangle_\nu+\langle a_\alpha(\varphi^{-1}\xi)\partial_{k_\beta}\psi_0\rangle_\nu]. \tag{105}$$

Solving Eq. (105) requires the knowledge of $\partial_{\mathbf{k}}\psi_0$ and of its adjoint which have been obtained in Eqs. (92) and (93). After substitution, we get the diffusion matrix as

$$D_{\alpha\beta}=-\frac{1}{2}\partial_{k_\alpha}\partial_{k_\beta}s_0=\frac{1}{2\langle T\rangle_\nu}\left\langle\sum_{j=-\infty}^{+\infty}a_\alpha(\xi)a_\beta(\varphi^j\xi)\right\rangle_\nu. \tag{106}$$

If diffusion is isotropic in the lattice, the diffusion matrix is diagonal $D_{\alpha\beta}=D\delta_{\alpha\beta}$ with the diffusion coefficient

$$D=\frac{1}{2L\langle T\rangle_\nu}\sum_{j=-\infty}^{+\infty}\langle\mathbf{a}(\xi)\cdot\mathbf{a}(\varphi^j\xi)\rangle_\nu, \tag{107}$$

which is a discrete version of the Green-Kubo relation [37,38]

$$D=\frac{1}{2L}\int_{-\infty}^{+\infty}\langle\mathbf{v}(X)\cdot\mathbf{v}(\Phi^t X)\rangle_\mu dt. \tag{108}$$

Equations (107) and (108) are strictly equivalent, as can be shown by a direct calculation using Eq. (14). Equation (107) is also another version of a formula obtained by Cvitanović, Eckmann, and Gaspard [28], which expresses the diffusion coefficient in terms of the unstable periodic orbits and their characteristic quantities appearing in the ζ function (59). In this formula of Ref. [28], the diffusion coefficient is given as the ratio of the autocorrelation function of the jump function to the average time of flight, both calculated from the stability eigenvalues of the mapping, i.e., from the invariant measure of the mapping.

E. Microscopic current and Fick's law

In order to show that our construction satisfies Fick's law, we need to calculate the mean current of particles passing by an arbitrary cell when the system is in the nonequilibrium steady state given by Eq. (100).

The outgoing and ingoing currents at the cell $\mathbf{l}$ are given by, respectively,

$$\mathbf{j}^{(\mathrm{out})}=\tfrac{1}{2}\langle\mathbf{v}(\xi,\tau)\Psi_{\mathbf{g}}(\xi,\tau,\mathbf{l})\rangle_\mu \tag{109}$$

and

$$\mathbf{j}^{(\mathrm{in})}=\tfrac{1}{2}\langle\mathbf{v}(\theta\xi,\tau)\Psi_{\mathbf{g}}(\xi,\tau,\mathbf{l})\rangle_\mu, \tag{110}$$

where we took the time-reversed velocity. The factor $\frac{1}{2}$ is required because each cell of the suspension flow contains particles in transit between two lattice sites.

We first remark that the term linearly increasing with $\mathbf{l}$ in (100) is constant in each cell of the lattice so that this term vanishes in the mean currents. Therefore $\Psi_{\mathbf{g}}$ can be replaced by $\psi_{\mathbf{g}}$ in Eqs. (109) and (110). Using the definition (21) of the invariant measure together with Eqs. (14) and (94), as well as the time-reversal properties (22) and (23), we get

$$\mathbf{j}^{(\mathrm{out})}=-\frac{1}{2\langle T\rangle_\nu}\sum_{j=1}^{\infty}\langle\mathbf{a}(\xi)\mathbf{g}\cdot\mathbf{a}(\varphi^{-j}\xi)\rangle_\nu+\frac{1}{2\langle T\rangle_\nu}\langle\mathbf{n}(\xi)\mathbf{g}\cdot\mathbf{a}(\varphi^{-1}\xi)\rangle_\nu, \tag{111}$$

$$\mathbf{j}^{(\mathrm{in})}=+\frac{1}{2\langle T\rangle_\nu}\sum_{j=0}^{\infty}\langle \mathbf{a}(\xi)\mathbf{g}\cdot\mathbf{a}(\varphi^j\xi)\rangle_\nu + \frac{1}{2\langle T\rangle_\nu}\langle \mathbf{n}(\xi)\mathbf{g}\cdot\mathbf{a}(\varphi^{-1}\xi)\rangle_\nu . \tag{112}$$

Finally, the total current is

$$\mathbf{j}^{(\mathrm{tot})}=\mathbf{j}^{(\mathrm{out})}-\mathbf{j}^{(\mathrm{in})}=-\frac{1}{2\langle T\rangle_\nu}\sum_{j=-\infty}^{+\infty}\langle \mathbf{a}(\xi)\mathbf{g}\cdot\mathbf{a}(\varphi^j\xi)\rangle_\nu = -D\mathbf{g}, \tag{113}$$

where we used the assumption that diffusion is isotropic according to Eq. (107). Equation (113) shows that the current corresponding to the nonequilibrium steady state $\Psi_{\mathbf{g}}$ obeys Fick's law. A similar result has been obtained for the multibaker by Tasaki and Gaspard [30,31].

VI. HIGHER-ORDER DIFFUSION COEFFICIENTS

In this section we investigate the higher-order derivatives of the eigenvalue and of the eigenstates with respect to the wave number. We show that these derivatives are related to higher-order diffusion coefficients such as the Burnett coefficients which appear at the fourth order [39]. If the dispersion relation of diffusion is expanded in Taylor series around $\mathbf{k}=\mathbf{0}$ we obtain

$$s_{\mathbf{k}}=-D_{\alpha\beta}k_\alpha k_\beta+B_{\alpha\beta\gamma\delta}k_\alpha k_\beta k_\gamma k_\delta+O(k^6). \tag{114}$$

$D_{\alpha\beta}$ is the matrix of the diffusion coefficients and $B_{\alpha\beta\gamma\delta}$ is the tensor containing the Burnett coefficients, which are thus given by the fourth derivatives of the eigenvalue with respect to the wave number at $\mathbf{k}=\mathbf{0}$.

To simplify the calculations, we make use of a formal solution of the eigenvalue problem. Thereafter, we observe that taking N derivatives with respect to the wave number leads to sums involving at most N-time correlation functions of the characteristic functions $T(\xi)$ and $\mathbf{a}(\xi)$ of the system with respect to the mapping φ.

Here, the assumption that the mapping has the K property becomes essential. Indeed, the K property is known to imply the K mixing [40] and, as a consequence, the property of multiple mixing that the multiple correlation functions decay as

$$\langle f_0(\xi)f_1(\varphi^{j_1}\xi)f_2(\varphi^{j_2}\xi)\ldots f_{N-1}(\varphi^{j_{N-1}}\xi)\rangle_\nu \rightarrow\langle f_0\rangle_\nu\langle f_1\rangle_\nu\langle f_2\rangle_\nu\ldots\langle f_{N-1}\rangle_\nu \tag{115}$$

for $|j_m-j_n|\rightarrow\infty$ for all $m,n=1,\ldots,N-1$ and for piecewise Hölder continuous functions f_m. The bound (15) on the decay of the two-time correlation functions implies that

$$|\langle f_0(\xi)f_1(\varphi^{j_1}\xi)\ldots f_{N-1}(\varphi^{j_{N-1}}\xi)\rangle_\nu|\leqslant C(f_0,f_1,\ldots,f_{N-1})\mathrm{Min}_{1\leqslant m<n\leqslant N-1}\{\exp(-|j_m-j_n|^\gamma)\}, \tag{116}$$

if $\langle f_m\rangle_\nu=0$ and where C is a positive constant. Therefore the sums of such N-time correlation functions over the integers j_m are guaranteed to converge. Under such circumstances, higher-order diffusion coefficients such as the Burnett coefficients exist in the system.

A. Formal solution to the eigenvalue problem

A formal solution of the eigenvalue equation (65) can be obtained by applying successively the Frobenius-Perron operator to the unit function to get

$$\psi_{\mathbf{k}}(\xi)=\lim_{n\rightarrow\infty}\prod_{j=1}^{n}\exp[-s_{\mathbf{k}}T(\varphi^{-j}\xi)-i\mathbf{k}\cdot\mathbf{a}(\varphi^{-j}\xi)] =\lim_{n\rightarrow\infty}\exp\Xi_{\mathbf{k}}^{(n)}. \tag{117}$$

By Eqs. (69) and (72), we obtain the adjoint eigenvector as

$$\tilde{\psi}_{\mathbf{k}}(\xi)=\lim_{n\rightarrow\infty}\prod_{j=0}^{n-1}\exp[-s_{\mathbf{k}}^*T(\varphi^{j}\xi)+i\mathbf{k}\cdot\mathbf{a}(\varphi^{j}\xi)] =\lim_{n\rightarrow\infty}\exp\tilde{\Xi}_{\mathbf{k}}^{(n)}. \tag{118}$$

The normalization condition (67) becomes an eigenvalue equation to determine $s_{\mathbf{k}}$

$$1=\langle\tilde{\psi}_{\mathbf{k}}^*\psi_{\mathbf{k}}\rangle_\nu =\lim_{n\rightarrow\infty}\left\langle\prod_{j=-n}^{+n-1}\exp[-s_{\mathbf{k}}T(\varphi^j\xi)-i\mathbf{k}\cdot\mathbf{a}(\varphi^j\xi)]\right\rangle_\nu =\lim_{n\rightarrow\infty}\langle\exp\Gamma_{\mathbf{k}}^{(n)}\rangle_\nu . \tag{119}$$

The derivatives of the eigenvalue $s_{\mathbf{k}}$ can therefore be obtained by differentiating successively (119) with respect to the wave number and setting $\mathbf{k}=\mathbf{0}$.

The three first derivatives yield the known results that

$$\partial_{k_\alpha}s_0=\lim_{n\rightarrow\infty}\frac{1}{2n\langle T\rangle_\nu}\sum_{j=-n}^{+n-1}\langle a_\alpha(\varphi^j\xi)\rangle_\nu=0, \tag{120}$$

$$\partial_{k_\alpha}\partial_{k_\beta}s_0=\lim_{n\rightarrow\infty}-\frac{1}{2n\langle T\rangle_\nu}\sum_{i=-n}^{+n-1}\sum_{j=-n}^{+n-1}\langle a_\alpha(\varphi^j\xi)a_\beta(\varphi^j\xi)\rangle_\nu = -2D_{\alpha\beta}, \tag{121}$$

$$\partial_{k_\alpha}\partial_{k_\beta}\partial_{k_\gamma}s_0=0. \tag{122}$$

Equation (121) implies Eq. (106) because of the identity

$$\sum_{i=-n}^{+n-1}\sum_{j=-n}^{+n-1} C(j-i)=\sum_{j=-2n+1}^{2n-1}(2n-|j|)C(j), \quad (123)$$

and of the property of fast decay of correlations.

B. Burnett coefficients

An expression for the Burnett coefficient can be obtained by differentiating Eq. (119) four times with respect to the wave number. The calculation is long but straightforward. It is necessary to introduce the quantity $\Delta T(\xi)=T(\xi)-\langle T\rangle_\nu$ in order for the average $\langle \Delta T\rangle_\nu$ to vanish so that the property (116) can be applied. In the calculation, the following correlation functions appear:

$$C=\frac{1}{\langle T\rangle_\nu}\sum_{i=-\infty}^{+\infty}\langle \Delta T(\xi)\Delta T(\varphi^i\xi)\rangle_\nu, \quad (124)$$

$$E_{\alpha\beta}=\frac{1}{\langle T\rangle_\nu}\sum_{i,j=-\infty}^{+\infty}\langle \Delta T(\xi)a_\alpha(\varphi^i\xi)a_\beta(\varphi^j\xi)\rangle_\nu, \quad (125)$$

$$F_{\alpha\beta\gamma\delta}=\frac{1}{\langle T\rangle_\nu}\sum_{i,j,k=-\infty}^{+\infty}[\langle a_\alpha(\xi)a_\beta(\varphi^i\xi)a_\gamma(\varphi^j\xi)a_\delta(\varphi^k\xi)\rangle_\nu-\langle a_\alpha(\xi)a_\beta(\varphi^i\xi)\rangle_\nu\langle a_\gamma(\varphi^j\xi)a_\delta(\varphi^k\xi)\rangle_\nu$$
$$-\langle a_\alpha(\xi)a_\gamma(\varphi^j\xi)\rangle_\nu\langle a_\beta(\varphi^i\xi)a_\delta(\varphi^k\xi)\rangle_\nu-\langle a_\alpha(\xi)a_\delta(\varphi^k\xi)\rangle_\nu\langle a_\beta(\varphi^i\xi)a_\gamma(\varphi^j\xi)\rangle_\nu]. \quad (126)$$

The fourth derivatives of the eigenvalues are now given by

$$\partial_{k_\alpha}\partial_{k_\beta}\partial_{k_\gamma}\partial_{k_\delta}s_0=F_{\alpha\beta\gamma\delta}+4C(D_{\alpha\beta}D_{\gamma\delta}+D_{\alpha\gamma}D_{\beta\delta}+D_{\alpha\delta}D_{\beta\gamma})$$
$$-2(D_{\alpha\beta}E_{\gamma\delta}+D_{\alpha\gamma}E_{\beta\delta}+D_{\alpha\delta}E_{\beta\gamma}+D_{\beta\gamma}E_{\alpha\delta}+D_{\beta\delta}E_{\alpha\gamma}+D_{\gamma\delta}E_{\alpha\beta}) \quad (127)$$

and the Burnett coefficients by

$$B_{\alpha\beta\gamma\delta}=\frac{1}{4!}\partial_{k_\alpha}\partial_{k_\beta}\partial_{k_\gamma}\partial_{k_\delta}s_0. \quad (128)$$

In the case of isochronism ($\Delta T=0$), only the first term remains in Eq. (127) and we obtain a discrete version of a known formula for the Burnett coefficient [39]. However, in the absence of isochronism, correlations between the jump function and the return time function must also be taken into account, which explains the presence of the extra terms with C and $E_{\alpha\beta}$ in Eq. (127).

C. Eigenvalues and the Van Hove function

We already mentioned that Eq. (119) can be used to calculate the eigenvalue. If the return time function $T(\xi)$ presents bounded deviations around a positive and finite value, we may replace the sum over the times of flight by a given time t, and the sum over the jump vectors by the position vector traveled by the particle in the lattice over the time t. In this way, the eigenvalue is given by the alternative expression [15]

$$s_{\mathbf{k}}=\lim_{t\to\infty}\frac{1}{t}\ln\langle \exp i\mathbf{k}\cdot[\mathbf{r}(\Phi^tX)-\mathbf{r}(X)]\rangle_\mu=\lim_{t\to\infty}\frac{1}{t}\ln F(\mathbf{k},t), \quad (129)$$

in terms of the Van Hove incoherent intermediate scattering function

$$F(\mathbf{k},t)=\langle \exp i\mathbf{k}\cdot[\mathbf{r}(\Phi^tX)-\mathbf{r}(X)]\rangle_\mu, \quad (130)$$

which has been introduced in the study of diffusion by neutron or light scattering techniques [4]. In the form (129), we can recognize that the leading eigenvalue of the Frobenius-Perron operator is nothing else than the dispersion relation of diffusion. The diffusion coefficient can also be obtained from (129), leading to the well-known Einstein formula. Similarly, taking four derivatives of (129) with respect to $\mathbf{k}$ would give the Burnett coefficients in terms of a known continuous-time version of (126) [39].

D. The second derivative of the eigenstate with respect to the wave number

We may wonder if higher derivatives of the eigenstates with respect to the wave number also exist. Taking the first derivative of the formal solution (117), we obtain immediately the result (92) at the basis of the expression of the nonequilibrium steady states. In a similar way, the second derivative is given by

$$\partial_{k_\alpha}\partial_{k_\beta}\psi_{\mathbf{k}}(\xi)=\lim_{n\to\infty}\exp\Xi_{\mathbf{k}}^{(n)}(\partial_{k_\alpha}\partial_{k_\beta}\Xi_{\mathbf{k}}^{(n)}+\partial_{k_\alpha}\Xi_{\mathbf{k}}^{(n)}\partial_{k_\beta}\Xi_{\mathbf{k}}^{(n)}). \quad (131)$$

At $\mathbf{k}=\mathbf{0}$, we get

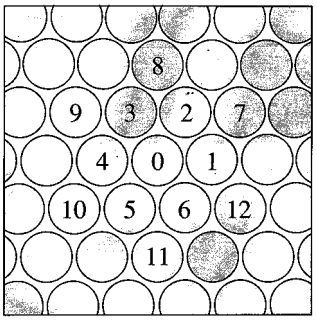

FIG. 2. Lorentz gas with a finite horizon showing the 12 disks to which transitions are allowed by the geometry starting from disk No. 0.

$$\partial_{k_\alpha}\partial_{k_\beta}\psi_0(\xi)=2D_{\alpha\beta}\sum_{j=1}^{\infty}T(\varphi^{-j}\xi)-\sum_{i=1}^{\infty}a_\alpha(\varphi^{-i}\xi)\sum_{j=1}^{\infty}a_\beta(\varphi^{-j}\xi). \quad (132)$$

Here again, this expression is meaningless as a function but may acquire a mathematical meaning as a distribution on test functions which are piecewise Hölder continuous and such that $\langle f\rangle_\nu=0$. The property of decay of multiple correlations (116) guarantees the expression $\langle f(\xi)\partial_{k_\alpha}\partial_{k_\beta}\psi_0(\xi)\rangle_\nu$ to converge. Therefore higher derivatives of the eigenstates with respect to the wave number may also be expected to exist as distributions.

VII. THE LORENTZ GAS AS A SUSPENSION FLOW

A. Definition of the dynamics

To illustrate the preceding theory, we consider the Lorentz gas where a point particle undergoes elastic collisions on hard disks which are fixed in the form of a triangular lattice in the plane. The disks are assumed to have a radius equal to unity and we denote by d the distance between the centers of the disks. For this system, Bunimovich and Sinai proved the existence of a finite diffusion coefficient in the finite horizon regime when $2<d<4/\sqrt{3}$ (see Fig. 2) [9]. In contrast, for $d>4/\sqrt{3}$, the horizon affecting the particle as well as the diffusion coefficient becomes infinite and diffusion is anomalous. For $d<2$, the point particle remains trapped in one of the closed billiards formed at the interstices between the partially overlapping disks. Here below, we consider the finite horizon regime where diffusion is normal [24].

The point particle moves in the plane and collides with fixed hard disks. The position vector is $\mathbf{r}=(x,y)$. Elastic collisions occur on the disks which are impenetrable so that the allowed positions satisfy

$$\mathcal{Q}:|\mathbf{r}-\mathbf{l}_{mn}|>1, \quad (133)$$

where

$$\mathbf{l}_{mn}=m\mathbf{l}_{10}+n\mathbf{l}_{01}\in\mathcal{L} \quad (134)$$

are the positions of the centers of the disks. These vectors belong to the triangular Bravais lattice $\mathcal{L}$ defined in terms of the two basic vectors

$$\mathbf{l}_{10}=(d,0) \quad \text{and} \quad \mathbf{l}_{01}=\left(\frac{d}{2},\frac{\sqrt{3}}{2}d\right), \quad (135)$$

where m and n are two integers. Accordingly, the reciprocal lattice $\tilde{\mathcal{L}}$ introduced with the spatial Fourier transforms in Sec. III is also triangular with a hexagonal Brillouin zone of area (31) given by

$$|\mathcal{B}|=\frac{(2\pi)^2}{|\mathbf{l}_{10}\times\mathbf{l}_{01}|}=\frac{8\pi^2}{\sqrt{3}d^2}. \quad (136)$$

Between the collisions, the motion of the Lorentz gas is ruled by the free-particle Hamiltonian (28). The dynamics on the different energy shells only differ by a rescaling of the time in terms of the magnitude of the velocity $|\mathbf{v}|$. Therefore we can restrict ourselves without loss of generality to the energy shell where the velocities have a unit magnitude $|\mathbf{v}|=1$. On this energy shell, the phase space of the flow is tridimensional composed of the two positions $\mathbf{r}=(x,y)\in\mathcal{Q}$ and of the angle α of the velocity with respect to the x axis: (x,y,α). Accordingly, the velocity is given by $\mathbf{v}=|\mathbf{v}|(\cos\alpha,\sin\alpha)$ with $\alpha\in[0,2\pi[$.

Let us consider a trajectory $[\mathbf{r}(t),\mathbf{v}(t)]$. In the phase space, the trajectory is piecewise linear between the collisions. At each collision $\{t_j\}_{j=-\infty}^{+\infty}$, the current position satisfies $|\mathbf{r}(t_j)-\mathbf{l}_j|=1$, where $\mathbf{l}_j$ is the center of the disk where the collision takes place. The velocities before and after the jth collision are denoted, respectively, by $\mathbf{v}_j^{(-)}$ and $\mathbf{v}_j^{(+)}$. Denoting the points of impact on the disks by $\{\mathbf{r}_j\}_{j=-\infty}^{+\infty}$, the vector normal to the disk and exterior to the disk at the jth collision is given by

$$\mathbf{n}_j=\frac{\mathbf{r}_j-\mathbf{l}_j}{|\mathbf{r}_j-\mathbf{l}_j|}=\mathbf{r}_j-\mathbf{l}_j. \quad (137)$$

With these definitions, the velocities before and after each collision are related according to the law of geometric optics

$$\mathbf{v}_j^{(+)}=\mathbf{v}_j^{(-)}-2\mathbf{n}_j(\mathbf{n}_j\cdot\mathbf{v}_j^{(-)}), \quad (138)$$

while the trajectory between the collisions is

$$\mathbf{r}(t)=\mathbf{r}_j+(t-t_j)\mathbf{v}_j^{(+)} \quad \text{for } t_j\leqslant t\leqslant t_{j+1}. \quad (139)$$

These equations define the flow in the phase space given by the domain $\mathcal{Q}$ of the billiard and by the range $[0,2\pi[$ of the velocity angle.

B. Suspension flow

The collision rule (138) and the trajectory equation (139) allow us to reduce the flow of the Lorentz gas to its Birkhoff mapping, as follows.

Each collision is uniquely characterized by the disk $\mathbf{l}_j$ of the collision, by the arc of perimeter r_j of the impact, and by the angle η_j between the outgoing velocity $\mathbf{v}_j^{(+)}$ and the normal at the point of impact $\mathbf{n}_j:\mathbf{n}_j\cdot\mathbf{v}_j^{(+)}=\cos\eta_j\geqslant 0$. The

Birkhoff coordinates $(r_j, v_j) \in \mathscr{P}$ are given by the aforementioned arc of perimeter r_j starting from the x axis and by the velocity component v_j parallel to the border of the disk,

$$v_j = \mathbf{t}_j \cdot \mathbf{v}_j^{(+)} = \sin\eta_j . \tag{140}$$

$\mathbf{t}_j$ is a unit vector tangent to the disk at the point of impact such that $\mathbf{t}_j \cdot \mathbf{n}_j = 0$ and the basis $(\mathbf{n}_j \mathbf{t}_j)$ has the same orientation as the axes (x,y).

The motion from a collision to the next is thus given by the Birkhoff mapping $\xi_{j+1} = \varphi(\xi_j)$ which is area preserving so that condition (I) and Eq. (18) are satisfied. Moreover, condition (II) holds for the mapping φ which is time-reversal symmetric under the involution $\theta(r,v) = (r,-v)$ satisfying (22).

The first return time function $T(\xi)$ is here given by the time of flight between two successive collisions,

$$T(\xi_j) = |\mathbf{r}_{j+1} - \mathbf{r}_j| , \tag{141}$$

which is equivalent to the length of the corresponding free path since $|\mathbf{v}| = 1$. On the other hand, the jump function $\mathbf{a}(\xi)$ is given by a vector of the triangular Bravais lattice (134) and (135). With these definitions, we can construct the mapping (9), which controls the suspension flow of the Lorentz gas. Introducing the time coordinate τ between two successive collisions, the complete set of coordinates of the suspension flow is here explicitly given by

$$\begin{aligned} X = (\xi, \tau, \mathbf{l}) &= (r, v, \tau, \mathbf{l}) \\ &\in [0, 2\pi[\otimes]-1, +1[\otimes [0, T(\xi)[\otimes \mathscr{L} . \end{aligned} \tag{142}$$

The original flow can be reconstructed from these coordinates thanks to Eq. (13) where the vector $\mathbf{n}(\xi)$ is the normal vector (137). From the knowledge of the Birkhoff coordinates and of the current disk, the position and velocity of the particle at the collision can thus be recovered according to

$$\begin{aligned} \mathbf{n}_j &= (\cos r_j, \sin r_j), \\ \mathbf{t}_j &= (-\sin r_j, \cos r_j), \\ \mathbf{r}_j &= (\cos r_j, \sin r_j) + \mathbf{l}_j , \\ \mathbf{v}_j^{(+)} &= [\cos(r_j + \eta_j), \sin(r_j + \eta_j)] \\ &= [\sqrt{1 - v_j^2} \cos r_j - v_j \sin r_j , \\ &\quad \sqrt{1 - v_j^2} \sin r_j + v_j \cos r_j]. \end{aligned} \tag{143}$$

During the flights between the collisions, the isomorphism between the coordinates (142) and the original coordinates of the particle is hence given by

$$\Sigma(r, v, \tau, \mathbf{l}) = \left[\mathbf{l} + \begin{pmatrix} \cos r + \tau \cos\alpha \\ \sin r + \tau \sin\alpha \end{pmatrix}, \begin{pmatrix} \cos\alpha \\ \sin\alpha \end{pmatrix} \right] = (\mathbf{r}, \mathbf{v}), \tag{144}$$

where

$$\begin{aligned} \cos\alpha &= \cos(r + \eta) = \sqrt{1 - v^2} \cos r - v \sin r , \\ \sin\alpha &= \sin(r + \eta) = \sqrt{1 - v^2} \sin r + v \cos r . \end{aligned} \tag{145}$$

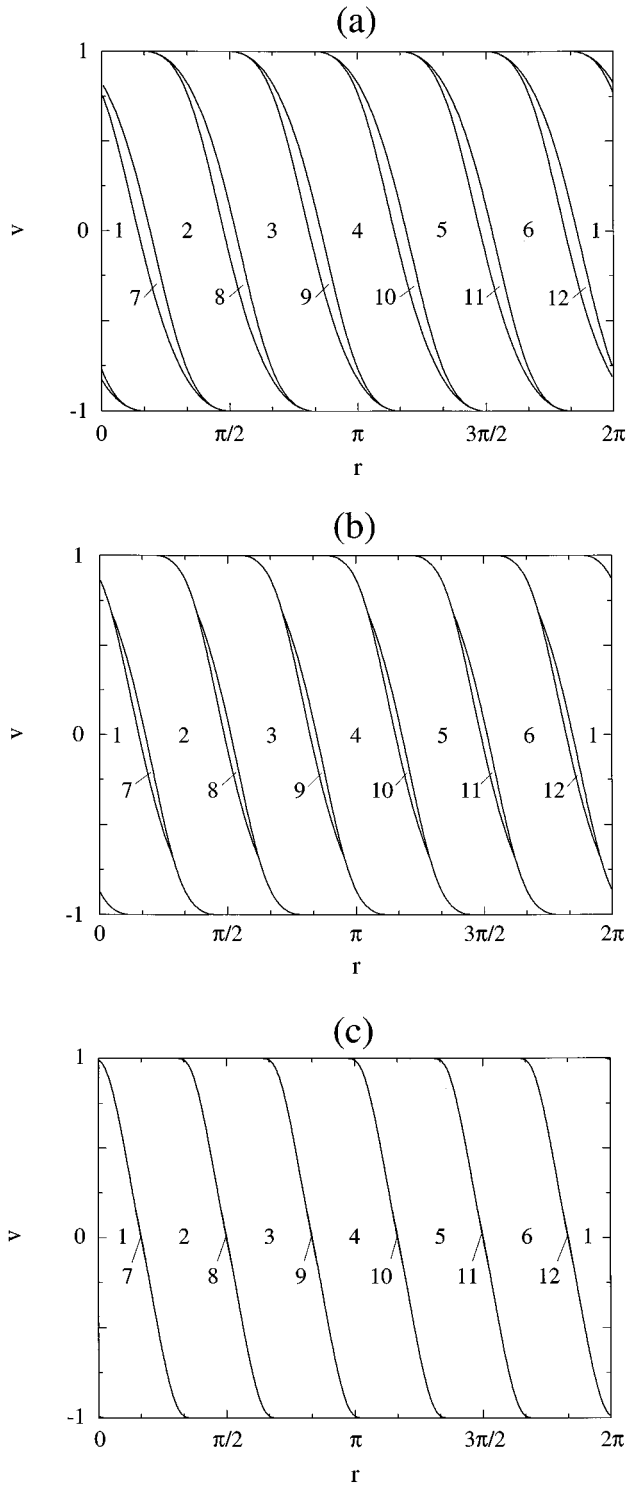

FIG. 3. In the coordinates $\xi = (r,v) \in [0, 2\pi[\otimes]-1, +1[$, representation of the lines of discontinuities of the mapping φ separating the subdomains (146): (a) for $d = 2.3$; (b) for $d = 2.15$; (c) for $d = 2.01$. The integers are the labels l of the disks reached at the next collision, assuming that the particle is initially on the disk No. 0, as shown in Fig. 2.

C. Properties of the mapping

Here, we summarize some known properties of the Birkhoff mapping of the Lorentz gas [9–11,24].

In the case of a finite horizon, the particle on the disk at the origin can only move to one of the 12 disks of the first and second shells surrounding the central disk (see Fig. 2).

Therefore the domain of definition of the mapping φ is divided into 12 subdomains

$$\mathscr{P}=[0,2\pi[\otimes]-1,+1[=\cup_{l=1,\ldots,12}\mathscr{P}_l. \tag{146}$$

Examples of such subdomains are given in Fig. 3. On the borders $\partial\mathscr{P}_l$ of these subdomains, each one of the functions $\varphi(\xi)$, $T(\xi)$, and $\mathbf{a}(\xi)$ defining the mapping (9) is discontinuous. Inside the subdomains $\mathscr{P}_l$, these functions are smooth, i.e., analytic. In particular, for $\xi\in\mathscr{P}_l$, the jump vector $\mathbf{a}(\xi)$ is constant since it is given by the vector between the centers of the disks 0 and l.

The dynamical instability of the Lorentz gas can be characterized by the largest Lyapunov exponent. For the trajectory of initial condition $X=(\xi,\tau,\mathbf{l})$, this latter is obtained as

$$\lambda(X)=\lim_{T\to+\infty}\frac{1}{T}\int_0^T B_u(\phi^t X)dt, \tag{147}$$

where the curvature of the expanding horocircle accompanying the trajectory (as defined in Ref. [35]) is given by [10]

$$B_u(\xi,\tau)=\cfrac{1}{\tau+\cfrac{1}{\cfrac{2}{\sqrt{1-v_0^2}}+\cfrac{1}{T_{-1}+\cfrac{1}{\cfrac{2}{\sqrt{1-v_{-1}^2}}+\cfrac{1}{T_{-2}+\cfrac{1}{\cfrac{2}{\sqrt{1-v_{-2}^2}}+\cdots}}}}}}, \tag{148}$$

where $0\leqslant\tau\leqslant T(\xi)$, $T_j=T(\varphi^j\xi)$, and $v_j=v(\varphi^j\xi)$ with $j=0,-1,-2,-3,\ldots$. The expanding horocircle is determined by the past trajectory. Because the curvature (148) is positive for all the trajectories when the horizon is finite, the Lyapunov exponent of each trajectory is also positive and the dynamics is hyperbolic. The first part of condition (III) is therefore satisfied.

The curvatures immediately before and after the collision at ξ are defined by, respectively,

$$B_u^{(-)}(\xi)=B_u[\varphi^{-1}\xi,T(\varphi^{-1}\xi)], \tag{149}$$

$$B_u^{(+)}(\xi)=B_u(\xi,0). \tag{150}$$

According to the ergodic property proved by Bunimovich and Sinai [9], the average Lyapunov exponent is thus given in terms of the ergodic invariant measure μ as

$$\overline{\lambda}=\langle B_u(\xi,\tau)\rangle_\mu=\frac{1}{\langle T\rangle_\nu}\int\frac{dr\,dv}{4\pi}\int_0^{T(\xi)}d\tau\,\frac{1}{\tau+\cfrac{1}{B_u^{(+)}(\xi)}}$$

$$=\frac{1}{\langle T\rangle_\nu}\langle\ln[1+T(\xi)B_u^{(+)}(\xi)]\rangle_\nu, \tag{151}$$

which is a form of the Abramov formula [19].

Furthermore, the tangent space of the area-preserving mapping φ can be decomposed locally into its stable and unstable directions. The unstable direction at $\xi=(r,v)$ is given by [10]

$$\frac{dv_u}{dr}=\sqrt{1-v^2}[B_u^{(-)}(r,v)\sqrt{1-v^2}+1], \tag{152}$$

where

$$B_u^{(-)}(\xi)=\cfrac{1}{T_{-1}\cfrac{1}{\cfrac{2}{\sqrt{1-v_{-1}^2}}+\cfrac{1}{T_{-2}+\cfrac{1}{\cfrac{2}{\sqrt{1-v_{-2}^2}}+\cfrac{1}{T_{-3}+\cfrac{1}{\cfrac{2}{\sqrt{1-v_{-3}^2}}+\cdots}}}}}}, \tag{153}$$

with the same conventions as in Eq. (148). On the other hand, the stable direction is given by

$$\frac{dv_s}{dr} = -\sqrt{1-v^2}[B_s^{(+)}(r,v)\sqrt{1-v^2}+1], \qquad (154)$$

in terms of the curvature $B_s^{(+)}(\xi)$ of the contracting horocircle, which is determined by an expression similar to (153) but for the whole future trajectory (with T_{-j} replaced by T_{j-1} and v_{-j} by v_j).

The stable and unstable directions exist at every point ξ of the domain of definition of the mapping. Nevertheless, the stable and unstable directions have discontinuities inherited from the discontinuities of the mapping. These discontinuities of the curvatures appear on a dense set of zero Lebesgue measure because all the images or preimages of the borders of the subdomains, namely, $\varphi^j(\partial\mathscr{P}_l)$, form discontinuities. This phenomenon is shown in Fig. 4. Because of these discontinuities, the dynamics is not structurally stable so that the disk billiard is not an Axiom-A system.

In spite of these differences with respect to Axiom-A systems, Bunimovich and Sinai [9] and, more recently, Chernov and co-workers [10,11] proved for the Lorentz gas the series of ergodic properties which we require in condition (III).

(a) The Lorentz gas is a K flow so that it is K mixing, mixing, and ergodic [9].

(b) The decay of correlations with respect to the mapping is fast of stretched exponential type so that (15) is satisfied for piecewise Hölder continuous functions [11].

(c) The central limit theorem (16) and (17) holds [9–11].

(d) When the Lorentz gas has a finite horizon, both the functions $T(\xi)$ and $\mathbf{a}(\xi)$ are bounded and the central limit theorem applies to them so that the diffusion coefficient is positive and finite and the trajectories follow a standard Brownian process on large scales [9].

Since conditions (I)–(III) hold for the regular Lorentz gas with a finite horizon, we can apply the spectral theory of the Frobenius-Perron operator to construct the nonequilibrium steady states, the hydrodynamic modes, and the dispersion relation of diffusion as a Pollicott-Ruelle resonance.

D. Nonequilibrium steady states

In Sec. V we constructed the nonequilibrium steady states corresponding to a gradient $\mathbf{g}$ of concentration in the form of Eq. (94). Thanks to the results of Chernov [11], we obtain the following theorem.

Theorem. In the triangular Lorentz gas with finite horizon, the nonequilibrium steady state $\psi_{\mathbf{g}}(\xi)$ is a distribution or linear functional defined by Eq. (96) on piecewise Hölder continuous functions $f(\xi)$ defined on the domain (146).

This result can be proved using the property (15) of fast decay of correlations which applies to the jump vector $\mathbf{a}(\xi)$ since it is bounded and piecewise Hölder continuous. Considering a test function $f(\xi)$ which is also piecewise Hölder continuous, the series (96) thus converges absolutely, which defines the nonequilibrium steady state as a linear functional. Q.E.D.

Since the forward dynamics tends to smooth out the probability densities along the unstable directions the corresponding invariant measure $\psi_{\mathbf{g}}(\xi)$ given by (94) is regular along the unstable directions (152) but singular along the stable directions (154). For the flow of the Lorentz gas, the nonequilibrium steady state may be obtained from Eq. (102), in which the first term is a regular function which represents the average linear profile of concentration across the lattice. On the other hand, it is the second term which is singular and which represents the fluctuations around the nonequilibrium steady state.

In order to give a representation to a distribution like (94) we consider its cumulative function defined by applying the distribution on the characteristic function

$$\chi_{(r,v)}(\xi) = \begin{cases} 1 & \text{for } \xi \in [0,r[\otimes]-1,v[\\ 0 & \text{otherwise,} \end{cases} \qquad (155)$$

which is also piecewise Hölder continuous. The cumulative function of the nonequilibrium steady state is therefore defined as

$$\mathscr{T}_{\mathrm{g}}(r,v) = \langle \chi_{(r,v)}\psi_{\mathbf{g}}\rangle_\nu = \frac{1}{4\pi}\int_0^r dr' \int_{-1}^{v} dv'\, \psi_{\mathbf{g}}(r',v'), \qquad (156)$$

which has two components whether the gradient is in the x or in the y direction,

$$\mathscr{T}_x(r,v) = -\sum_{j=1}^{\infty} \langle \chi_{(r,v)}(\xi) a_x(\varphi^{-j}\xi)\rangle_\nu ,$$

$$\mathscr{T}_y(r,v) = -\sum_{j=1}^{\infty} \langle \chi_{(r,v)}(\xi) a_y(\varphi^{-j}\xi)\rangle_\nu , \qquad (157)$$

so that $\mathscr{T}_{\mathbf{g}} = g_x\mathscr{T}_x + g_y\mathscr{T}_y$. These functions, which are continuous but nondifferentiable, are the analog for the Lorentz gas of the nonequilibrium steady state constructed by Tasaki and Gaspard for the dyadic multibaker [30,31].

The functions (157) are depicted in Figs. 5 and 6 for two different values of the interdisk distance. In the Lorentz gas, the particle performs several collisions in each cell before going to neighboring cells and diffusing. On the contrary, in the multibaker, the particle immediately goes to a neighboring cell after one iteration. For this reason, the fractal nature of the curves defined by the cumulative functions is less apparent in the Lorentz gas than in the multibaker.

E. Diffusion and its dispersion relation

In Sec. V we showed that the leading Pollicott-Ruelle resonance of the Frobenius-Perron operator (55) gives us the dispersion relation of diffusion. In particular, the diffusion coefficient is obtained from the second derivative of the eigenvalue $s_{\mathbf{k}}$ with respect to the wave number at $\mathbf{k}=\mathbf{0}$. Since the triangular lattice is isotropic, the diffusion coefficient is given by Eq. (107) with $L=2$.

The eigenvalue itself can be obtained using the Van Hove function (130) and Eq. (129), which we used for a numerical evaluation of the dispersion relation depicted in Fig. 7. We observe that the eigenvalue satisfies

$$s_{\mathbf{k}} \simeq -Dk^2, \qquad (158)$$

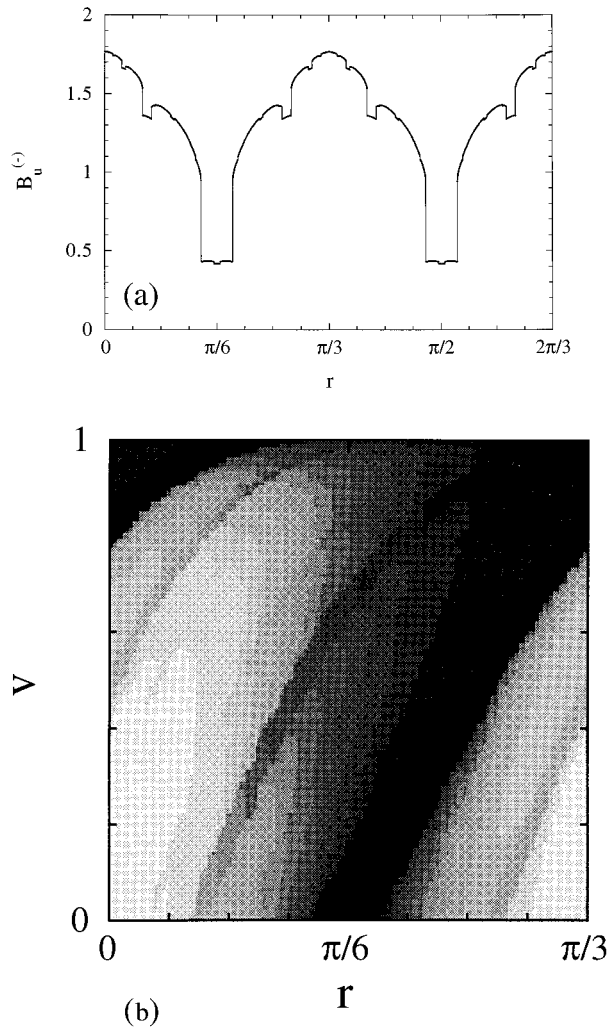

FIG. 4. In the Lorentz gas with $d=2.3$: (a) Curvature $B_u^{(-)}$ of the unstable horocircle immediately before the collision given by Eq. (153) along the line $\xi=(r,v=0)$ (dots; a solid line joining the dots is used to display the discontinuities). (b) Density plot of $B_u^{(-)}$ in the domain where $0<r<\pi/3$ and $0<v<1$. The instability is higher in the light regions than in the dark ones. The preimages of the discontinuity lines appear in this plot. The first preimages are the discontinuities of the inverse mapping φ^{-1} which are the lines of Fig. 3 transformed by the time-reversal symmetry under $(r,v)\to(r,-v)$.

at small values of the wave number $\mathbf{k}$. The value of the diffusion coefficient obtained by this method is in agreement with the values previously obtained by other methods [12,24]. No deviation with respect to (158) has been observed at small wave numbers beyond numerical errors so that the Burnett coefficients should be very small. At larger values of $\mathbf{k}$, the eigenvalue $s_{\mathbf{k}}$ seems to encounter other singularities down along the negative real axis which suggests that the dispersion relation becomes either complex or ill defined due to complex singularities, for instance, branch cuts.

F. Cumulative functions of the eigenstates

We have also investigated numerically the properties of the eigenstates, solutions of Eq. (65), by using the formal

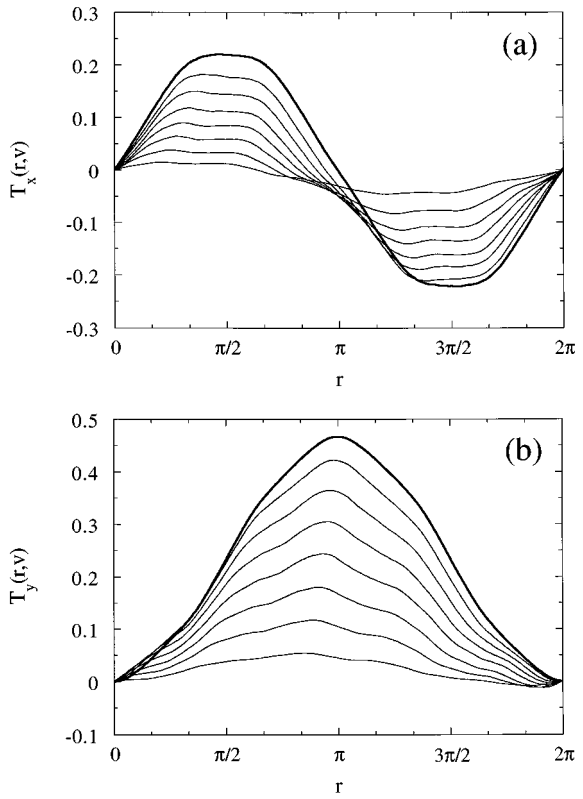

FIG. 5. In the Lorentz gas with $d=2.3$, representation of the nonequilibrium steady states given by their cumulative functions (157): (a) $\mathscr{T}_x(r,v)$ for a gradient along the x axis; (b) $\mathscr{T}_y(r,v)$ for a gradient along the y axis. The cumulative functions are plotted in the interval $0<r<2\pi$ for fixed values of $v=-0.75$, -0.5, -0.25, 0, 0.25, 0.5, 0.75, and 1.

solution given by (117). As for the nonequilibrium steady states, the distributions defining the eigenstates can also be represented by their cumulative functions as

$$\mathscr{G}_{\mathbf{k}}(r,v)=\langle\chi_{(r,v)}\psi_{\mathbf{k}}\rangle_\nu, \tag{159}$$

in terms of the characteristic function (155). The real and imaginary parts of these complex functions are depicted in Fig. 8. Expanding the eigenstate in Taylor series around $\mathbf{k}=\mathbf{0}$, the cumulative function becomes

$$\begin{aligned}\mathscr{G}_{\mathbf{k}}(r,v)&=\langle\chi_{(r,v)}\rangle_\nu+\mathbf{k}\cdot\langle\chi_{(r,v)}\partial_{\mathbf{k}}\psi_0\rangle_\nu\\&\quad+\frac{1}{2}\mathbf{k}\mathbf{k}:\langle\chi_{(r,v)}\partial_{\mathbf{k}}^2\psi_0\rangle_\nu+O(k^3)\\&=\frac{r(v+1)}{4\pi}+i\mathscr{T}_{\mathbf{g}=\mathbf{k}}(r,v)+O(k^2).\end{aligned} \tag{160}$$

We observe that the first term corresponds to the uniform probability density representing the microcanonical ensemble ν for which the cumulative function is real and linear in the coordinates $r\in[0,2\pi[$ and $v\in]-1,+1[$. The second term is precisely the cumulative function (156) and (157) of the nonequilibrium steady state here evaluated for $\mathbf{g}=\mathbf{k}$. We notice that the real part is determined by all the even derivatives while the imaginary part is determined by all the odd derivatives. Therefore we have

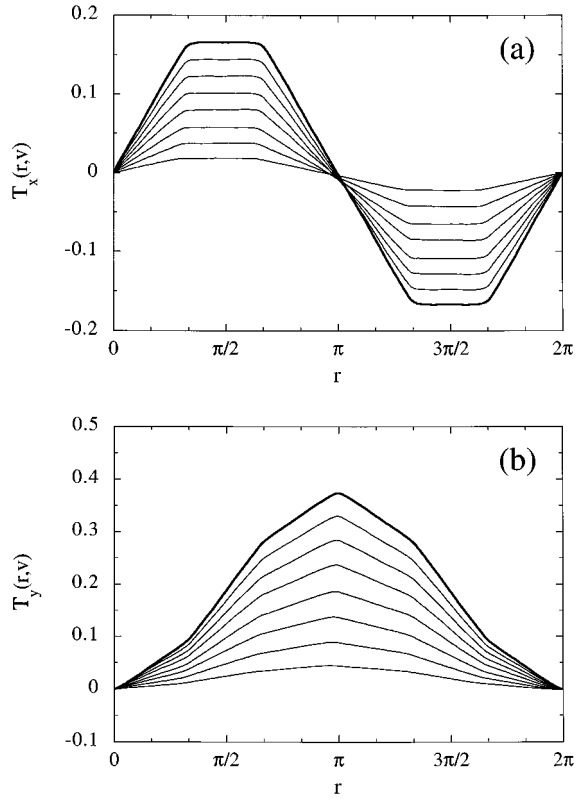

FIG. 6. Same as Fig. 5 in the Lorentz gas with $d=2.01$.

$$\mathrm{Re}\mathscr{G}_{\mathbf{k}}(r,v)=\frac{r(v+1)}{4\pi}+O(k^2),$$

$$\mathrm{Im}\mathscr{G}_{\mathbf{k}}(r,v)=\mathscr{T}_{\mathbf{g}=\mathbf{k}}(r,v)+O(k^3), \tag{161}$$

in accordance with the real and imaginary parts of the eigenstates of Fig. 8, as compared with the nonequilibrium steady state of Fig. 5. This comparison illustrates that the nonequilibrium steady state provides the leading contribution to the imaginary part of the eigenstate which is a numerical evidence of the consistency of the theory.

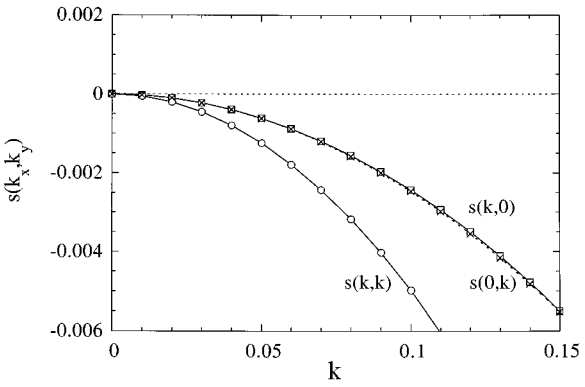

FIG. 7. In the Lorentz gas with $d=2.3$, dispersion relation of diffusion $s_{\mathbf{k}}=s(k_x,k_y)$ given by Eq. (129) in terms of the Van Hove function. The eigenvalue is evaluated along $\mathbf{k}=(k,0)$ (squares, solid line); $\mathbf{k}=(0,k)$ (crosses, dashed line); $\mathbf{k}=(k,k)$ (circles, solid line). The three curves are consistent with $s_{\mathbf{k}}\simeq -D(k_x^2+k_y^2)$ with the diffusion coefficient $D\simeq 0.25$. We remark that the eigenvalue $s_{\mathbf{k}}$ presents a small imaginary part (not visible in the figure) due to numerical errors.

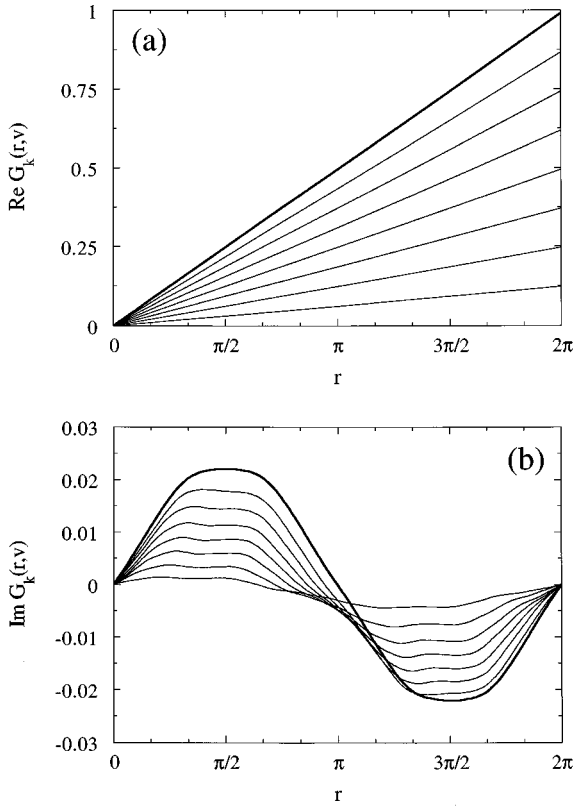

FIG. 8. In the Lorentz gas with $d=2.3$, eigenstate $\psi_{\mathbf{k}}$ corresponding to a hydrodynamic mode of wave number $\mathbf{k}=(0.1,\ 0)$ and represented by its cumulative function $\mathscr{G}_{\mathbf{k}}(r,v)$ given by Eqs. (159)–(161): (a) real and (b) imaginary parts depicted in the interval $0<r<2\pi$ for fixed values of $v=-0.75$, -0.5, -0.25, 0, 0.25, 0.5, 0.75, and 1.

VIII. CONCLUSIONS

In this paper we constructed the hydrodynamic modes of diffusion in a large class of spatially extended flows, which includes Hamiltonian flows. The hydrodynamic modes are shown to be the eigenstates of the Frobenius-Perron operator associated with the Pollicott-Ruelle resonances. Moreover, we also deduced the nonequilibrium steady states corresponding to uniform gradients of concentration. Under the validity of several conditions, we showed that the nonequilibrium steady states have a mathematical meaning as distributions thanks to the property of decay of correlations. We prove this result for the Lorentz gas with a finite horizon in which the required conditions are known to hold.

The construction is based on the Pollicott-Ruelle eigenvalue problem for a special Frobenius-Perron operator of the mapping associated with the suspension flow. This Frobenius-Perron operator is obtained by two successive reductions. The first one uses a spatial Fourier transform to go from the lattice to one of its elementary cells while the second one uses the property that the flow is essentially controlled by a Poincaré mapping:

$$(\xi,\tau,\mathbf{l})\to(\xi,\tau|\mathbf{k})\to(\xi|s,\mathbf{k}),\qquad(162)$$

$$\hat{P}^t\to\hat{Q}^t_{\mathbf{k}}\to\hat{R}_{\mathbf{k},s},$$

which shows the chain of reductions. The last Frobenius-Perron operator is special because, on the one hand, it reduces the dynamics of the flow to a dynamics induced by the mapping, while, on the other hand, it depends on the wave number associated with the modes in the infinitely extended system.

The present work shows that this special Frobenius-Perron operator may admit eigenstates corresponding to exponential relaxation toward thermodynamic equilibrium. An explanation is here in order. Many recent works have been concerned by relaxation in the sector of vanishing wave number $\mathbf{k}=\mathbf{0}$ which is important for the decay of correlations. In this sector, the leading Pollicott-Ruelle resonance vanishes, $s_0=0$, and corresponds to the invariant Lebesgue measure ν of the microcanonical ensemble. In this sector, the decay of correlations is controlled by the complex singularities of the ζ function (59) deeper in the complex s plane below the leading Pollicott-Ruelle resonance $s_0=0$. These singularities which are not known for the moment lead in general to nonexponential decays of correlation functions in the sector $\mathbf{k}=\mathbf{0}$.

In contrast, we are here concerned by the *leading* Pollicott-Ruelle resonance, but in the sectors with nonvanishing wave numbers $\mathbf{k}\neq\mathbf{0}$. This problem has not yet been systematically studied. It turns out that there exists a leading Pollicott-Ruelle resonance $s_{\mathbf{k}}$ which is the continuation of the resonance $s_0=0$ as the wave number becomes nonvanishing. This resonance characterizes an exponential relaxation to the thermodynamic equilibrium because it is negative. Since $s_{\mathbf{k}}$ is arbitrarily small as $\mathbf{k}\to\mathbf{0}$, the relaxation rate becomes arbitrarily long as expected for hydrodynamic modes of diffusion when their wavelength increases. It is therefore not surprising to find well-defined exponential behaviors at the level of the special Frobenius-Perron operator which incorporates the wave number $\mathbf{k}$.

When $\mathbf{k}\neq\mathbf{0}$, the corresponding eigenstates are no longer absolutely continuous with respect to the Lebesgue measure but become singular measures or distributions defined on some smooth enough test functions. The distributions are sufficiently regular to admit cumulative functions which we plotted for the Lorentz gas.

The construction of the eigenstates we propose is systematic and is not approximate so that it constitutes a construction of the hydrodynamic modes—which describe an exponential relaxation to thermodynamic equilibrium—at the fundamental level of the Liouvillian dynamics. Moreover, our derivation of the Green-Kubo relation from the Ruelle-Pollicott resonance of the Frobenius-Perron operator provides a fundamental justification of this famous relation in terms of the dynamics of relaxation to the thermodynamic equilibrium. The Burnett coefficients are also justified in the same way.

In the present theory, the time evolution splits into two distinct semigroups corresponding to forward and backward evolutions of nonequilibrium statistical ensembles represented by smooth enough probability densities ρ. The Pollicott-Ruelle resonances with $\mathrm{Re}s_{\mathbf{k}}\leqslant 0$ are part of the forward semigroup defined for $t>0$. An antiresonance with $\mathrm{Re}\tilde{s}_{\mathbf{k}}\geqslant 0$ corresponds to each Pollicott-Ruelle resonance by time-reversal symmetry, which defines the backward semigroup of application for the negative times $t<0$. The eigenstates of the forward semigroup are smooth in the unstable directions but singular in the stable direction, but the situation is reversed for the backward semigroup. In this regard, the present theory provides an explanation of the phenomenon of irreversibility at the level of the time evolution of nonequilibrium statistical ensembles composed of infinitely many trajectories and represented by smooth probability densities ρ. Irreversibility has here its origin in the dynamical instability of the trajectories. This irreversibility at the statistical level of ensemble dynamics turns out to be compatible with the microscopic reversibility at the level of individual trajectories.

On the other hand, the present construction of the nonequilibrium steady states shows that the steady states are directly connected with the Green-Kubo relation and with the validity of Fick's law. Here, we see that the nonequilibrium steady states appear at the level of the first derivatives with respect to the wave number and the Green-Kubo relation at the level of the second derivatives.

The present work extends a previous construction by Tasaki and Gaspard [30,31] of the nonequilibrium steady states for the multibaker which are hence recovered. Indeed, the multibaker mapping is given by the area-preserving baker map in the coordinates $\xi=(x,y)$ so that the return time function may be taken as $T(\xi)=1$. In the multibaker, transport occurs along a sequence of squares as described by the function $a(\xi)=\mp 1$ whether the jump is to the left or to the right depending on whether $0<x<1/2$ or $1/2<x<1$. In this case, the nonequilibrium steady state (100) is given by

$$\Psi_g(\xi,l)=gl-\sum_{j=1}^{\infty} ga(\varphi^{-j}\xi).\qquad(163)$$

Its cumulative function,

$$\mathcal{T}_g(\xi,l)=\int_0^x dx'\int_0^y dy'\,\Psi_g(x',y',l)=glxy+gxT(y),\qquad(164)$$

involves the so-called Takagi function $T(y)$, which is continuous but nondifferentiable and has fractal properties. In the case of the Lorentz gas, Eq. (157) defines therefore the analog of the Takagi function in an infinitely extended billiard.

As we discussed elsewhere [23,25], nonequilibrium invariant measures with fractal supports can be used to define nonequilibrium states in the chaotic-scattering approach. In this approach, the fractal support tends to fill the whole phase space and becomes a plain support in the infinite-system limit. In this way, the nonequilibrium measures and escape-time functions of the chaotic-scattering approach turn out to be related to the present nonequilibrium steady state as shown explicitly for the multibaker [31].

The simplicity of the expressions (102) and (103) of the nonequilibrium steady states suggests the generalization of the present results to the other transport and rate coefficients in N-particle systems. Let us suppose that the gradient cor-

responding to the transport coefficient α is given by the unit vector $\mathbf{g}$. The microscopic current corresponding to such a process is denoted by $J_{\mathbf{g}}^{(\alpha)}$. A Helfand moment $G_{\mathbf{g}}^{(\alpha)}$ is associated with the microscopic current such that $J_{\mathbf{g}}^{(\alpha)}=(d/dt)G_{\mathbf{g}}^{(\alpha)}=\{G_{\mathbf{g}}^{(\alpha)},H\}$, where $\{\ ,\ \}$ denotes the Poisson bracket [41]. In the case of diffusion $G_{\mathbf{g}}^{(D)}=\mathbf{g}\cdot\mathbf{r}$ and $J_{\mathbf{g}}^{(D)}=\mathbf{g}\cdot\mathbf{v}$ where $\mathbf{r}$ and $\mathbf{v}$ are the particle position and velocity [23]. The nonequilibrium steady state and its time-reversed state are thus given in general systems by

$$\Psi_{\mathbf{g}}^{(\alpha)}(X)=G_{\mathbf{g}}^{(\alpha)}(X)+\int_0^{-\infty}J_{\mathbf{g}}^{(\alpha)}(\Phi^t X)dt, \tag{165}$$

$$\tilde{\Psi}_{\mathbf{g}}^{(\alpha)}(X)=G_{\mathbf{g}}^{(\alpha)}(X)+\int_0^{+\infty}J_{\mathbf{g}}^{(\alpha)}(\Phi^t X)dt \tag{166}$$

for a trajectory of initial condition at the phase-space point $X=\{\mathbf{R}_a,\mathbf{P}_a\}_{a=1}^N$. We should notice that the distributions (165) and (166) are invariants of motion in the sense that $\Psi_{\mathbf{g}}^{(\alpha)}(X)=\Psi_{\mathbf{g}}^{(\alpha)}(\Phi^t X)$, as can be verified using the definitions of $G_{\mathbf{g}}^{(\alpha)}$ and $J_{\mathbf{g}}^{(\alpha)}$. This invariance is rendered compatible with the presence of chaotic behaviors thanks to the singular character of the states. Indeed, a theorem by Moser asserts that there are no analytic invariant functions in the presence of transverse homoclinic orbits as is the case here [42]. The presence of chaotic behaviors thus opens the way to new types of invariant of motion given by distributions.

The average current in the direction $\mathbf{e}$ is given as one-half the outgoing flux minus one-half the ingoing flux, which can be calculated with the time-reversed steady state in analogy with the case of diffusion treated here above,

$$\begin{aligned} j_{\mathbf{e}}^{(\alpha)}&=\tfrac{1}{2}\langle J_{\mathbf{e}}^{(\alpha)}(X)\Psi_{\mathbf{g}}^{(\alpha)}(X)\rangle_\mu-\tfrac{1}{2}\langle J_{\mathbf{e}}^{(\alpha)}(X)\tilde{\Psi}_{\mathbf{g}}^{(\alpha)}(X)\rangle_\mu \\ &=-\frac{1}{2}\int_{-\infty}^{+\infty}\langle J_{\mathbf{e}}^{(\alpha)}(X)J_{\mathbf{g}}^{(\alpha)}(\Phi^t X)\rangle_\mu dt=-\alpha\mathbf{e}\cdot\mathbf{g}, \end{aligned} \tag{167}$$

where $\langle\rangle_\mu$ denotes the average over the equilibrium state and where we used a change of variable $t\to -t$. This result is obtained for an isotropic system under the condition of validity of the Green-Kubo relations. The result (167) shows that the average current is constant and given by the unit gradient multiplied by the transport coefficient in agreement with Fick's and Fourier's laws, or the laws ruling viscosity. In this way, the methods of the present work can be used to construct nonequilibrium steady states associated with viscosity, in particular, in the two-disk fluid studied in Ref. [43].

After the completion of the present work, we learned that in the 1970s Zubarev introduced local integrals of motion of the form [44]

$$P^{(\alpha)}(\mathbf{x},t)=\rho^{(\alpha)}(\mathbf{x},t)+\int_{-\infty}^0\boldsymbol{\nabla}\cdot\mathbf{j}^{(\alpha)}(\mathbf{x},t+\tau)d\tau, \tag{168}$$

where $\rho^{(\alpha)}$ and $\mathbf{j}^{(\alpha)}$ are the local density and current associated with the property α and which obey the local conservation equation $\partial_t\rho^{(\alpha)}+\boldsymbol{\nabla}\cdot\mathbf{j}^{(\alpha)}=0$. In the case of diffusion, $\rho^{(D)}=\delta[\mathbf{x}-\mathbf{r}(t)]$ and $\mathbf{j}^{(D)}=\mathbf{v}(t)\,\delta[\mathbf{x}-\mathbf{r}(t)]$ so that Zubarev's local integral of motion turns out to be related to our invariant of motion (165) according to

$$\Psi_{\mathbf{g}}^{(D)}(\mathbf{r},\mathbf{v})=\int(\mathbf{g}\cdot\mathbf{x})P^{(D)}(\mathbf{x},0)d^3x, \tag{169}$$

as shown by a straightforward calculation using properties of the derivative of Dirac distribution, as well as $\mathbf{r}(0)=\mathbf{r}$ and $\mathbf{v}(0)=\mathbf{v}$. The present theory in which these invariants of motion are derived from the Liouville dynamics clarifies the interpretation of these quantities.

In conclusion, this work brings a microscopic foundation of the hydrodynamic modes and of the nonequilibrium steady states in a large class of continuous-time systems, including Hamiltonian flows. These modes which play a central role in kinetic theory turn out to be defined at the level of phase space in terms of mathematical distributions or, equivalently, of singular measures. As a consequence, the hydrodynamic modes and the nonequilibrium steady states cannot be represented in general by density functions but by cumulative functions in the case of a Liouville dynamics. The problem of the construction of the hydrodynamic modes has been a major preoccupation in kinetic theory since the works of Boltzmann and Hilbert [3,29]. This construction has been restricted to the level of the kinetic equations obtained after the introduction of some stochastic approximation which turns singular measures into regular ones. This approximate procedure seemed until very recently to be an inherent limitation in nonequilibrium statistical mechanics. However, we can see in the present work that such approximations can be avoided thanks to the recent developments in dynamical systems theory.

ACKNOWLEDGMENTS

P.G. would like to thank Professor G. Nicolis for support and encouragement in this research. The author also thanks Dr. S. Tasaki for inspiring discussions on nonequilibrium steady states and for pointing out to him Zubarev's work, Professor J. R. Dorfman who introduced him to Helfand's moments, as well as Professor L. Bunimovich for a discussion on K mixing. The author is grateful to the National Fund for Scientific Research (F.N.R.S. Belgium) and the ''Communauté française de Belgique'' (ARC Contract No. 93/98-166) for financial support.

[1] I. Prigogine, *Nonequilibrium Statistical Mechanics* (Wiley, New York, 1962).

[2] R. Balescu, *Equilibrium and Nonequilibrium Statistical Mechanics* (Wiley, New York, 1975).

[3] R. Résibois and M. De Leener, *Classical Kinetic Theory of Fluids* (Wiley, New York, 1977).

[4] J.-P. Boon and S. Yip, *Molecular Hydrodynamics* (Dover, New York, 1980).

[5] M. Pollicott, Invent. Math. **81**, 413 (1985).

[6] D. Ruelle, *Thermodynamic Formalism* (Addison-Wesley,

Reading, MA, 1978); D. Ruelle, *Chaotic Evolution and Strange Attractors* (Cambridge University Press, Cambridge, England, 1989).
[7] D. Ruelle, Phys. Rev. Lett. **56**, 405 (1986); J. Stat. Phys. **44**, 281 (1986).
[8] D. Ruelle, J. Differ. Geom. **25**, 99 (1987); **25**, 117 (1987).
[9] L. A. Bunimovich and Ya. G. Sinai, Commun. Math. Phys. **78**, 247 (1980); **78**, 479 (1980).
[10] Ya. G. Sinai and N. I. Chernov, Russ. Math. Surv. **42**, 181 (1987); L. A. Bunimovich, Ya. G. Sinai, and N. I. Chernov, *ibid.* **45**, 105 (1990).
[11] N. I. Chernov, J. Stat. Phys. **74**, 11 (1994).
[12] J. Machta and R. Zwanzig, Phys. Rev. Lett. **50**, 1959 (1983); J. Stat. Phys. **32**, 555 (1983).
[13] P. Gaspard, J. Stat. Phys. **68**, 673 (1992).
[14] P. Gaspard, Phys. Lett. A **168**, 13 (1992).
[15] P. Gaspard, Chaos **3**, 427 (1993).
[16] P. Gaspard, in *Dynamical Systems and Chaos*, edited by Y. Aizawa, S. Saito, and K. Shiraiwa (World Scientific, Singapore, 1995), Vol. 2, pp. 55–68.
[17] H. H. Hasegawa and D. J. Driebe, Phys. Rev. E **50**, 1781 (1994).
[18] C. Kittel, *Introduction to Solid State Physics* (Wiley, New York, 1976).
[19] J.-P. Eckmann and D. Ruelle, Rev. Mod. Phys. **57**, 617 (1985).
[20] A. Knauf, Commun. Math. Phys. **110**, 89 (1987).
[21] P. Gaspard and G. Nicolis, Phys. Rev. Lett. **65**, 1693 (1990).
[22] P. Gaspard and D. Alonso Ramirez, Phys. Rev. A **45**, 8383 (1992).
[23] J. R. Dorfman and P. Gaspard, Phys. Rev. E **51**, 28 (1995).
[24] P. Gaspard and F. Baras, Phys. Rev. E **51**, 5332 (1995).
[25] P. Gaspard and J. R. Dorfman, Phys. Rev. E **52**, 3525 (1995).
[26] N. Chernov and R. Markarian (unpublished).
[27] N. I. Chernov, G. L. Eyink, J. L. Lebowitz, and Ya. G. Sinai, Phys. Rev. Lett. **70**, 2209 (1993); Commun. Math. Phys. **154**, 569 (1993).
[28] P. Cvitanović, P. Gaspard, and T. Schreiber, Chaos **2**, 85 (1992); P. Cvitanović, J.-P. Eckmann, and P. Gaspard, Chaos Solitons Fractals **6**, 113 (1995).
[29] T. R. Kirkpatrick, E. G. D. Cohen, and J. R. Dorfman, Phys. Rev. A **26**, 950 (1982); **26**, 972 (1982); **26**, 995 (1982).
[30] S. Tasaki and P. Gaspard, in *Towards the Harnessing of Chaos*, edited by M. Yamaguti (Elsevier, Amsterdam, 1994), pp. 273–288.
[31] S. Tasaki and P. Gaspard, J. Stat. Phys. **81**, 935 (1995).
[32] D. Ruelle, *Elements of Differentiable Dynamics and Bifurcation Theory* (Academic Press, Boston, 1989).
[33] A function f is said to be piecewise Hölder continuous if $|f(\xi)-f(\xi')|\leqslant C(f)\|\xi-\xi'\|^{\beta}$ for both points ξ and ξ' belonging to a subdomain of a finite union of subdomains of $\mathscr{P}$, for some Hölder exponent $\beta>0$, and for some positive constant $C(f)$. The class of piecewise Hölder continuous functions is larger than the class of Hölder continuous functions defined on the same domain [11].
[34] B. O. Koopman, Proc. Natl. Acad. Sci. U.S.A. **17**, 315 (1931).
[35] V. I. Arnold and A. Avez, *Ergodic Problems of Classical Mechanics* (Benjamin, New York, 1968).
[36] R. Artuso, E. Aurell, and P. Cvitanović, Nonlinearity **3**, 325 (1990).
[37] M. S. Green, J. Chem. Phys. **19**, 1036 (1951); **20**, 1281 (1952); **22**, 398 (1954).
[38] R. Kubo, J. Phys. Soc. Jpn. **12**, 570 (1957); H. Mori, Phys. Rev. **112**, 1829 (1958).
[39] H. van Beijeren, Rev. Mod. Phys. **54**, 195 (1982).
[40] I. P. Cornfeld, S. V. Fomin, and Ya. G. Sinai, *Ergodic Theory* (Springer-Verlag, Berlin, 1982).
[41] E. Helfand, Phys. Rev. **119**, 1 (1960); Phys. Fluids **4**, 681 (1961).
[42] J. Moser, *Stable and Random Motions in Dynamical Systems* (Princeton University Press, Princeton, NJ, 1973).
[43] L. A. Bunimovich and H. Spohn, Commun. Math. Phys. (to be published).
[44] D. N. Zubarev, *Nonequilibrium Statistical Thermodynamics* (Consultants Bureau, New York, 1974).